Petrology, Vol. 11, No. 5, 2003, pp. 426–443. Translated from Petrologiya, Vol. 11, No. 5, 2003, pp. 471–490.

Riebeckite–Aegirine–Celadonite BIF at the Mikhailovskoe Iron Deposit of the Kursk Magnetic Anomaly: Phase Equilibria and Metamorphic Conditions

K. A. Savko and M. V. Poskryakova

Voronezh State University, Universitetskaya pl. 1, Voronezh, 394006 Russia
e-mail: gflab4@main.vsu.ru

Received August 10, 2002

Abstract—The Early Proterozoic banded iron formation (BIF) of the Mikhailovskoe iron deposit differs from other known Precambrian BIF by the low Al# and high $Fe^{3+}/(Fe^{3+} + Fe^{2+})$ ratios. The elevated oxygen fugacity during the metamorphic event and the Al-poor composition of the rocks were responsible for the origin of minerals high in Fe^{3+} and the absolute absence of Al-bearing phases. The BIF contains widespread celadonite, tetraferribiotite, Al-free chlorite, riebeckite, and aegirine instead of grunerite, stilpnomelane, minnesotaite, and greenalite, which are minerals usual in BIF elsewhere. Data on the phase equilibria provide information on the origin order of mineral assemblages and the physicochemical conditions of metamorphism. Its early stages were marked by the stability of quartz, carbonates, iron oxides, and potassic micas of specific composition. As the temperature increased, tetraferribiotite, celadonite, and riebeckite crystallized. Depending on the oxygen fugacity (above or below the hematite–magnetite buffer) in discrete layers, the *Aeg + Hem* and *Rbk + Mag* assemblages were formed. The metamorphic temperature was estimated at 370–520°C at a pressure of 2–3 kbar, Na activity $[\log[a(Na^+)/a(H^+)] = 5.5–6.0$, and oxygen fugacity above the hematite–magnetite buffer in layers with the *Aeg + Hem* assemblage and below this buffer in layers with *Rbk + Mag*.

INTRODUCTION

Banded iron formations (BIF) are an important constituent of all known Precambrian shields and the main indicator of the drastic change in the oxygen regime in the Earth's hydrosphere and atmosphere at the boundary between the Early and Late Proterozoic. Because of this, BIF were not found in complexes younger than 1.9 Ga. These unique Precambrian formations were studies by several researchers over many years. The main research avenues were the reconstruction of the sedimentation environments of the Fe-bearing rocks, analysis of their facies and formations, sources of the material, etc. At the same time, the evolution of BIF at the Kursk magnetic anomaly (KMA) was studied relatively poorly, mostly because of the following reasons:

* there is still no scheme of the facies and subfacies of Fe- and Si-rich rocks (contrary to, for example, metapelites);

* metamorphic zoning in rocks with such rare mineral assemblages was mapped very rarely (if at all);

* efforts to interpret the physicochemical metamorphic conditions of BIF were made based on very scarce experimental materials, particularly in the low- and medium-temperature regions, and these rocks contain no mineral assemblages that are conventionally utilized as geothermobarometers.

According to the chemical and mineralogic composition, BIF rocks are conventionally classed with one of the following four types of Fe–Si formations (James, 1954; Klein, 1973): (1) quartz–magnetite (hematite) type (which is also sometimes referred to as itabirite), containing the *Qtz–Mag*, *Qtz–Hem*, and *Qtz–Hem–Mag* assemblages; (2) quartz–carbonate, in which carbonates of the fero-dolomite–ankerite and siderite–pictomesite series are abundant; (3) quartz–silicate, which is dominated by quartz, Fe-rich phyllosilicates, such as greenalite, minnesotaite, chlorites (chamosite, clinochlore, ripidolite), micas (biotite, stilpnomelane, ferriannite), and, at higher metamorphic grades, grunerite, orthopyroxene, and fayalite; (4) Mn-rich BIF. Another type of widespread Early Proterozoic BIF at KMA are high-Fe riebeckite and aegirine-bearing rocks.

Thus, every type of high-Fe rocks is characterized by different mineral assemblages and, hence, their different evolutionary successions in the course of prograde metamorphism. Moreover, the stability of the mineral assemblages is strongly dependent on the oxygen fugacity, because of which a significant part in BIF metamorphism is played by redox reactions, which are particularly typical of low- and medium-temperature conditions. High-temperature metamorphism (to the high-temperature amphibolite and, particularly, granulite facies) of all of the aforementioned BIF types (except those high in Mn) results in magnetite–quartz–fayalite–orthopyroxene rocks, sometimes referred to as eulysites.

BIF rocks at the Mikhailovskoe iron deposit of KMA differ from other Precambrian BIF by low Al_2O_3 concentrations, even as compared with the generally low Al_2O_3 concentrations in all BIF rocks. This feature causes the complete absence of Al-bearing minerals. The phyllosilicates are K-bearing and virtually Al-free micas: celadonite and tetraferribiotite in place of stilpnomelane, minnesotaite, and greenalite, typical of BIF of low metamorphic grades. The wide occurrence of celadonite in association with tetraferribiotite, quartz, magnetite, and hematite at low metamorphic grades makes the Mikhailovskoe BIF different from other well-known Precambrian BIF at shields. The rocks also contain siderite, ankerite, Al-free chlorite, riebeckite, and aegirine.

This paper is centered on the succession of phase transitions in and the physicochemical metamorphic conditions of the tetraferribiotite–celadonite–riebeckite BIF at the Mikhailovskoe iron deposit, one of the largest in the world.

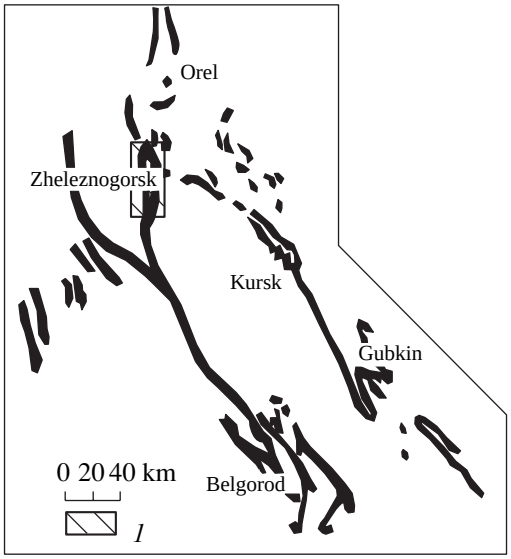

Fig. 1. Schematic map showing the distribution of the Early Proterozoic KMA BIF (after Shchegolev, 1985).
(*1*) Study area.

GEOLOGY

BIF were found in the KMA Precambrian at three stratigraphic levels: Early Archean, Late Archean, and Early Proterozoic. Archean BIF rocks occur locally, within small positive ellipsoidal, crescent-shaped, or stripe anomalies (Ushakovskoe, Kuvshinovskoe, Budanovskoe, Besedinskoe, and others) and consist of eulysites metamorphosed to the granulite facies. Their metamorphic parameters were assayed (Savko, 1999) at $T = 850°C$, $P = 5$ kbar, and $\log f_{O_2}$ from –14 to –15.

The Late Archean BIF rocks occur in greenstone belts in close association with amphibolites (Shchegolev, 1985). They compose elongated bodies up to 10 km long and relatively thin (no more than 100 m) and consist of quartz–magnetite–garnet–grunerite rocks. Their metamorphic parameters were determined at the Zapadnyi Kodentsovskii prospect as $T = 650 \pm 30°C$, $P = 5$ kbar, and $\log f_{O_2}$ from –17 to –20 (Savko, 1994).

The most widely spread BIF at KMA are of Early Proterozoic age (Kurskaya Group). The rocks compose two stripes (Shchigrovsko–Oskol'skaya and Mikhailovsko–Belomorskaya) trending roughly westward for more than 550 km (Fig. 1). All currently mined iron ores of KMA affiliate with the Early Proterozoic BIF.

We examined BIF rocks of the Mikhailovskoe ore field, whose central portion includes one of the worlds greatest Mikhailovskoe deposit (Fig. 2).

The deposit is hosted by Lower Proterozoic metamorphosed terrigenous–sedimentary rocks of the Kurskaya Group (Fig. 2). The group is subdivided into the sandy–shaly Stolenskaya and the BIF Korobkovskaya Formation. The Stoilenskaya Formation consists of a lower and upper subformations. In our study area, the rocks of the former are quartz conglomerates and quartz metasandstones with beds of almandine–chloritoid aluminous schists. The upper subformation consists of carbonaceous shales and barren quartzites. The Korobkovskaya Formation is subdivided into four subformations: lower iron-bearing, intermediate shaly, upper iron-bearing, and upper shaly. The lower iron-bearing subformation can be subdivided into four members: (1) magnetite quartzite, (2) magnetite–hematite quartzite, (3) hematite quartzite, and (4) intercalating magnetite and hematite quartzites.

BIF PETROGRAPHY AND CHEMISTRY

The rocks of the Korobkovskaya Formation at the Mikhailovskii mining district are dark gray and greenish gray fine-grained BIF, whose banding is accentuated by alternating mineralized (magnetite and hematite) and barren (quartz and silicate) layers (Fig. 3). The layers can have the following compositions: (a) quartz with magnetite, carbonate, and, sometimes, hematite (Borehole 3195); (b) hematite with quartz and, sometimes, magnetite, celadonite, and carbonates (sample MK-18); (c) silicate (riebeckite and celadonite) in association with hematite or magnetite (Boreholes 3830, 3829, 3291); and (d) magnetite with hematite, quartz, carbonates, and silicates (aegirine, riebeckite, and celadonite; Boreholes 3829, 3830, 3291). At the Mikhailovskoe Mine, BIF (which are sometimes plicated and crenulated) contain interbeds of variable composition: aegirine (up to 4 cm thick); aegirine–celadonite (up to 1.5–2 cm), riebeckite (0.5–1 cm), quartz–carbonate–celadonite (0.5–1 cm), magnetite (0.5–1 cm), and quartz–magnetite (1–2 cm) (Fig. 3).

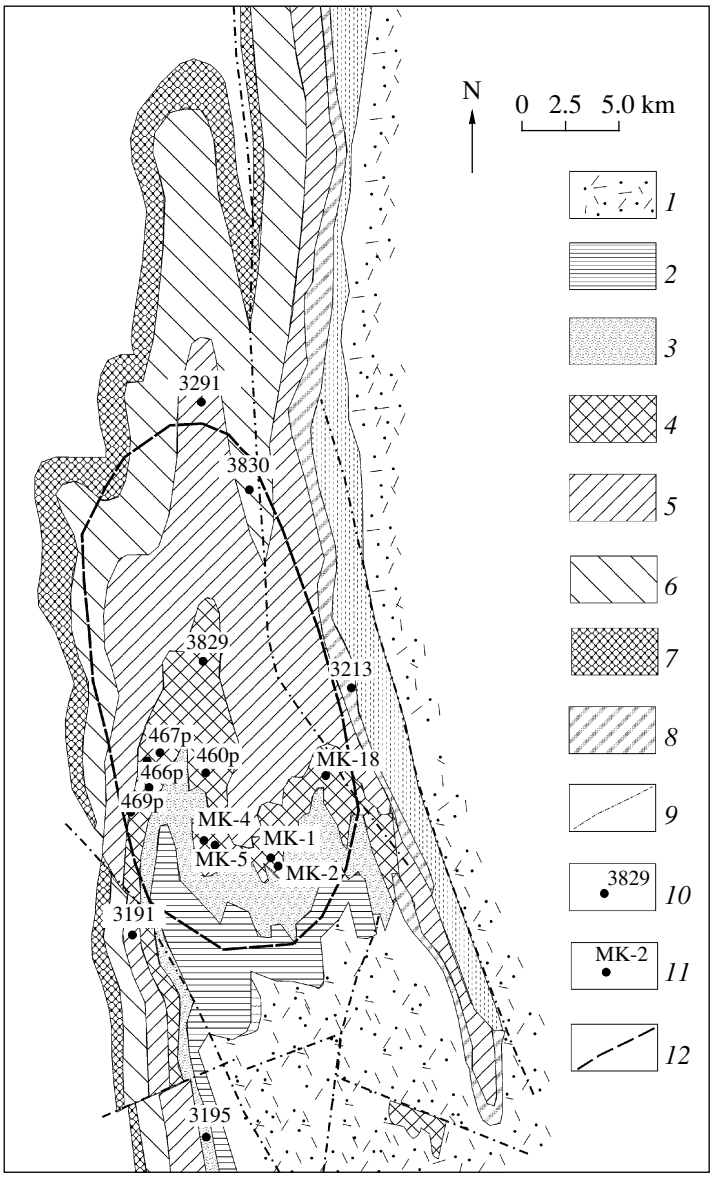

Fig. 2. Schematic geological map of the Mikhailovskoe iron deposit.

(*1*) Kurbakinskaya Formation: volcanomictic sandstone, shale, conglomerate, and quartz porphyry. Korobkovskaya Formation: (*2*) upper shale subformation (black carbonaceous quartz–chlorite–sericite shale), (*3*) upper iron ore subformation (magnetite, lean, red-banded hematite quartzite), (*4*) lower shale subformation (black carbonaceous quartz–chlorite–sericite shale and fine-grained sandstone), (*5*) lower iron ore subformation (magnetite and magnetite–hematite quartzite, red-banded hematite quartzite), (*6*) lower iron ore subformation, third unit (hematite–magnetite quartzite), (*7*) lower iron ore subformation, second unit (magnetite–hematite quartzite), (*8*) lower iron ore subformation, first unit (carbonate–magnetite, hematite–magnetite, and lean quartzite); (*9*) faults; (*10*) boreholes and their numbers; (*11*) sampling sites in the Mikhailovskii opencut mine; (*12*) contour of the Mikhailovskii opencut mine.

The mineralogy of BIF at the Mikhailovskoe iron deposit is controlled by the major-element chemistry and physicochemical metamorphic parameters. The chemistry of individual samples depends on the proportions of minerals composing the rocks. Chemical analyses of the Mikhailovskoe BIF are listed in Table 1 and generally correspond to the average composition of BIF from known iron-ore basins (Gole and Klein, 1981), except only for the FeO and Fe_2O_3 concentrations. The Mikhailovskoe BIF are noted for the strong predominance of Fe_2O_3 over FeO, with the $Fe^{3+}/(Fe^{3+} + Fe^{2+})$ ratios ranging from 0.70 to 0.87 (averaging 0.76) at elevated total Fe concentrations (ΣFe = 37.1–40.47 wt % at an average of 38.7 wt %). In a review of the chemical compositions of rocks from five Proterozoic BIF (Gole and Klein, 1981), the average value of the $Fe^{3+}/(Fe^{3+} + Fe^{2+})$ ratio does not exceed 0.5, ranging from 0.31 in the Marra Mamba Iron Formation in western Australia to 0.45–0.46 in formations of the Labrador Trough, Canada, and Biwabik in Minnesota, at total iron concentra-

tions of 30–32 wt %. Hence, the Mikhailovskoe BIF are characterized by a high average oxidation state of iron and its elevated overall concentrations compared with BIF elsewhere. The average K_2O and Na_2O concentrations in the rocks are closely similar to those in BIF in western Australia (Hamersley Basin, Marra Mamba) and are slightly higher than in BIF in North America.

We obtained microprobe analyses of minerals in the Early Proterozoic BIF from the Mikhailovskoe iron deposit. The mineral assemblages of these rocks are listed in Table 2, and the sampling sites are shown in Fig. 2.

METHODS

The more than 120 BIF samples are fragments of borehole core and specimens taken in the walls of the Mikhailovskoe opencut mine, which were described in much detail in field. The petrographic thin sections prepared from these samples were examined optically and analyzed at a Camebax SX-50 microprobe at the Moscow State University. The operating conditions were 15 kV accelerating voltage, 1–2 nA beam current, and 1–2 μm beam diameter. The analytical accuracy was systematically controlled by the analyses of natural and synthetic standards. The BSE images of thin sections were taken on a CamScan electron microscope with a Link EDS analytical set at the Moscow State University. The crystal chemical formulas of minerals were normalized to 6 oxygen atoms for aegirine, 23 for riebeckite, 11 for micas, 14 for chlorites, 8 for potassium feldspar, and 4 for magnetite.

Fig. 3. BIF at the sampling site MK-18 in the Mikhailovskii iron ore opencut mine.

Dark layers are magnetite–celadonite–riebeckite and magnetite–hematite–celadonite–aegirine BIF varieties.

MINERALOGY

Magnetite is the main ore- and rock-forming mineral and occurs as individual grains of various size and octahedral habit, which are commonly concentrated within thin layers and lamina up to a few millimeters thick. This mineral is present in virtually all rock types, and its amount attains 50 modal %. The composition corresponds to pure magnetite, with the MgO, MnO, SiO_2, and Al_2O_3 admixtures amounting to no more than a few tenths of a percent (Table 3).

Hematite is always quantitatively subordinate to magnetite and occurs as platelets and flakes ranging from fractions of a millimeter to a few millimeters. Small hematite flakes are usually grouped within thin lamina up to a few millimeters thick, which are parallel to the rock bedding.

Table 1. Chemical composition of BIF from the Mikhailovskoe deposit

Component	712	714	715	716/1	716/2	717/1	717/2	718/1	718/2	719	720	801
SiO_2	38.76	38.30	40.74	39.76	39.10	39.06	42.34	40.38	39.62	38.72	38.16	38.06
TiO_2	0.49	0.23	0.25	0.25	0.30	0.35	0.30	0.25	0.27	0.47	0.46	0.47
Al_2O_3	0.01	0.56	0.57	0.53	0.49	0.53	0.65	0.49	0.47	0.01	0.13	0.01
Fe_2O_3	50.26	43.18	39.44	39.40	45.40	38.91	35.90	38.26	42.77	43.90	44.91	41.88
FeO	6.85	11.42	12.50	13.41	10.34	13.69	13.65	14.21	11.05	11.58	11.49	14.06
MnO	0.01	0.03	0.05	0.02	0.02	0.03	0.03	0.03	0.02	0.02	0.03	0.02
MgO	0.35	1.08	1.04	1.18	0.61	1.24	1.24	1.25	1.08	1.07	0.11	1.42
CaO	1.59	0.78	0.91	0.98	0.77	1.26	1.24	1.21	0.98	1.13	1.08	1.19
Na_2O	0.04	0.30	0.38	0.85	0.20	0.55	0.40	0.55	0.37	0.48	0.35	0.61
K_2O	0.30	0.93	1.10	1.08	0.80	1.20	1.22	0.85	0.83	1.05	0.80	0.97
Total	98.66	96.81	96.98	97.46	98.03	96.82	96.97	97.48	97.46	98.43	98.52	98.69
ΣFe	40.47	39.08	37.31	37.98	39.79	37.85	35.72	37.81	38.50	39.71	40.43	40.22
$Fe^{3+}/(Fe^{3+} + Fe^{2+})$	0.87	0.77	0.74	0.73	0.80	0.72	0.70	0.71	0.78	0.77	0.78	0.73

Note: Analyses were conducted at the chemical laboratory of NPO Tsentrgeologiya.

Table 2. Mineralogic composition of BIF from the Mikhailovskoe deposit

Mineral	*Qtz*	*Mag*	*Hem*	*Sld*	*Bt*	*Chl*	*Ank*-Fe-*Dol*	*Sd*	*Aeg*	*Rbk*
MK-1	+	+	+	+	+	–	+	+	+	*
MK-2	+	+	+	+	–	+	–	–	–	+
MK-4	+	+	+	+	–	+	–	–	+	*
MK-5	+	+	+	+	–	–	+	+	+	–
MK-15	+	+	+	+	–	–	+	+	+	–
MK-18	+	+	+	+	–	–	–	–	+	–
3195/15	+	+	–	+	–	–	+	+	+	+
3213/8	+	+	+	+	+	+	+	+	+	*
3291/479	+	+	+	+	+	–	–	–	–	–
3829/2	+	+	+	+	s.g.	+	+	+	+	s.g.
3829/4	+	+	+	*	+	–	–	inc.	+	inc.
3829/6	+	+	+	+	s.g.	+	+	+	–	–
3829/7	+	+	+	+	–	–	–	+	+	inc., *
3830/14	+	+	+	+	–	–	+	+	+	–
3830/16	+	+	+	+	–	–	+	+	+	–
3830/21	+	+	–	+	+	–	–	–	–	+
3830/23	+	+	+	+	+	s.g.	+	+	–	+
3830/28	+	+	+	+	–	–	–	–	–	+
3830/29	+	+	+	+	inc.	–	+	+	+	*
3830/30	+	+	+	+	+	–	+	+	+	–
3830/31	+	+	+	–	+	+	–	–	–	+
3830/32	+	+	+	+	+	–	+	+	–	+
3830/39	+	+	+	+	+	+	+	+	+	–
3830/40	+	+	+	+	inc.	inc.	–	–	+	*
3830/47	+	+	+	+	inc.	+	+	+	+	inc.
3830/49	+	+	+	+	–	+	+	+	+	–
3830/58	+	+	–	+	–	–	+	+	–	+
3830/59	+	+	+	–	–	–	+	+	+	–
460p/86	+	+	+	+	–	–	+	+	+	–
466p/32	+	+	+	+	–	+	–	–	–	+
466p/100	+	+	–	+	–	+	+	+	–	+
466p/130	+	+	+	+	–	+	+	+	–	+
466p/131	+	+	+	+	inc.	inc.	+	+	+	–
467p/195	+	+	+	–	–	+	+	+	–	+
467p/205	+	+	+	–	–	+	+	+	+	–
467p/214	+	+	–	+	–	–	–	–	–	+
467p/217	+	+	+	–	–	+	+	+	–	+
469p/254	+	+	+	+	–	–	–	–	–	–

Note: Abbreviations: s.g—single grain, inc.—inclusion in aegirine; *secondary.

In addition to quartz and magnetite, hematite is usually accompanied by aegirine and phyllosilicates. Most samples show evidence of magnetite martitization, i.e., its replacement by pseudomorphs of secondary hematite.

Micas. The Mikhailovskoe BIF contain Fe-rich micas, which are either the only or the predominant silicates of most BIF varieties. We identified tetraferribiotite and celadonite.

Table 3. Chemical composition of carbonates and magnetite in BIF from the Mikhailovskoe deposit

Component	3830/58				3830/14			MK-18	3195/15	3291/479	460p/86.0		466p/131.0	
	Mag-7	*Dol*-8*	*Sd*-10	*Ank*-51	*Mag*-49	*Sd*-24	*Dol*-29	*Mag*-26	*Dol*-71	*Mag*-9	*Sd*-8	*Dol*-15	*Dol*-13	*Sd*-21
SiO_2	0.07	0.24	0.14	0.28	1.32	0.17	0.43	1.08	0.41	0.11	0.26	0.24	0.31	0.09
TiO_2	–	0.04	–	–	–	–	0.14	–	–	–	–	–	–	–
Al_2O_3	0.09	0.26	0.2	0.11	–	–	–	0.18	–	–	0.13	–	0.02	–
FeO	99.74	19.46	64.99	37.05	97.29	66.64	22.61	98.15	21.22	99.57	73.34	23.98	24.65	76.60
MnO	0.02	0.6	1.39	0.5	–	0.24	0.03	–	0.72	0.09	2.03	0.90	1.08	1.24
MgO	–	26.78	32.9	14.28	0.34	32.04	25.74	0.09	25.92	0.02	23.11	24.04	23.61	21.40
CaO	0.02	52.55	0.36	47.38	0.06	0.68	50.52	–	51.68	–	0.46	50.14	50.20	0.28
Na_2O	–	–	–	–	–	0.23	0.24	0.05	0.05	–	0.61	0.37	0.08	0.35
K_2O	–	0.07	0.01	0.01	–	–	0.07	0.15	–	–	0.03	0.30	–	–
Total	99.94	100.00	100.00	100.00	99.01	100.00	99.99	99.70	100.00	99.98	99.97	99.97	99.95	99.96
Si	0.03	–	–	–	0.05	–	–	0.04	–	–	–	–	–	–
Al	0.04	–	–	–	–	–	–	0.01	–	–	–	–	–	–
Ti	–	–	–	–	–	–	–	–	–	–	–	–	–	–
Fe^{3+}	1.90	–	–	–	1.90	–	–	1.95	–	1.01	–	–	–	–
Fe^{2+}	1.03	0.14	0.51	0.29	1.03	0.53	0.17	0.97	0.16	0.97	0.62	0.18	0.19	0.66
Mn	–	–	0.01	–	–	–	–	–	0.01	–	0.02	0.01	0.01	0.01
Mg	–	0.35	0.46	0.20	0.02	0.46	0.34	0.01	0.34	–	0.35	0.32	0.32	0.32
Ca	–	0.49	–	0.49	–	0.01	0.48	–	0.49	–	0.01	0.48	0.48	–
Na	–	–	–	–	–	–	–	0.02	–	0.22	0.01	0.01	0.01	–
K	–	–	–	–	–	–	–	0.01	–	–	–	–	–	–
X_{Fe}		0.29	0.53	0.59		0.54	0.33		0.32		0.64	0.36	0.37	0.67

* All analyses are normalized to 100%. Here and in Tables 4–7, dashes mean concentration below the analytical determination limit, n.a.—not analyzed; $X_{Fe} = Fe^{2+}/(Fe^{2+} + Mg)$; oxides are given in wt %.

Tetraferribiotite is a fairly rare Al-free mica, which has the formula $K(Mg, Fe^{2+}, Fe^{3+})_3[Fe^{3+} Si_3O_{10}](OH)_2$ and was discovered in 1955 during an unsuccessful experimental effort to synthesize K–OH amphibole (Veres *et al.*, 1955). One member of the tetraferribiotite group, ferriannite, was obtained in the experiments of Wones (1963) within the temperature range of 400–850°C, pressures of 1035–2070 bar, and an oxygen fugacity between the hematite–magnetite and iron–wuestite buffers. Wones explored the hypothesis that mica of ferriannite composition should occur in magmatic Fe-rich rocks. Later ferriannite was described in riebeckite-bearing rocks in iron formations in western Australia (Miyano and Miyano, 1982; Miyano, 1982) and South Africa (Miyano and Beukes, 1997). Micas of the tetraferriannite–tetraferriphlogopite isomorphous series were described in the iron formation of the Kursk Magnetic Anomaly as early as the 1950–1960s (Sudovikova, 1956; Illarionov, 1965).

Tetraferribiotite occurs in the iron formation of the Mikhailovskoe mining district in the form of small brownish flakes 0.2–1.0 mm across (Fig. 4b) approximately in every fourth sample, in which it is accompanied by magnetite, hematite, riebeckite, aegirine, celadonite, and carbonate. The mineral occurs in subordinate amounts compared with celadonite and is preferably localized in magnetite–hematite layers as disseminated flakes, although can occasionally also compose nearly monomineralic thin layers with merely minor amounts of celadonite and iron oxides. Tetraferribiotite sometimes forms inclusions in aegirine (Figs. 5a, 5d, 6a), although these rocks may contain no this mineral in the groundmass. When in magnetite–hematite layers, tetraferribiotite is commonly replaced by celadonite (Fig. 4b).

Tetraferribiotite in the KMA iron formation is less aluminous (Table 4; Al_2O_3 = 0.68–0.76 wt %) and more magnesian (MgO = 10.13–14.09 wt %) than natural ferriannite (Miyano and Miyano, 1982; Miyano and Beukes, 1997), whose Al_2O_3 content is always higher than 1.3 wt %, usually about 4–5 wt %, and the MgO concentration varies from 3.5 to 12.5 wt % (Fig. 7). The Si/Al ratio of the tetraferribiotite is always one order of magnitude higher: 3.0. The least aluminous tetraferribiotite was detected as inclusions in aegirine. Hence, the compositions of the KMA tetraferribiotite are most

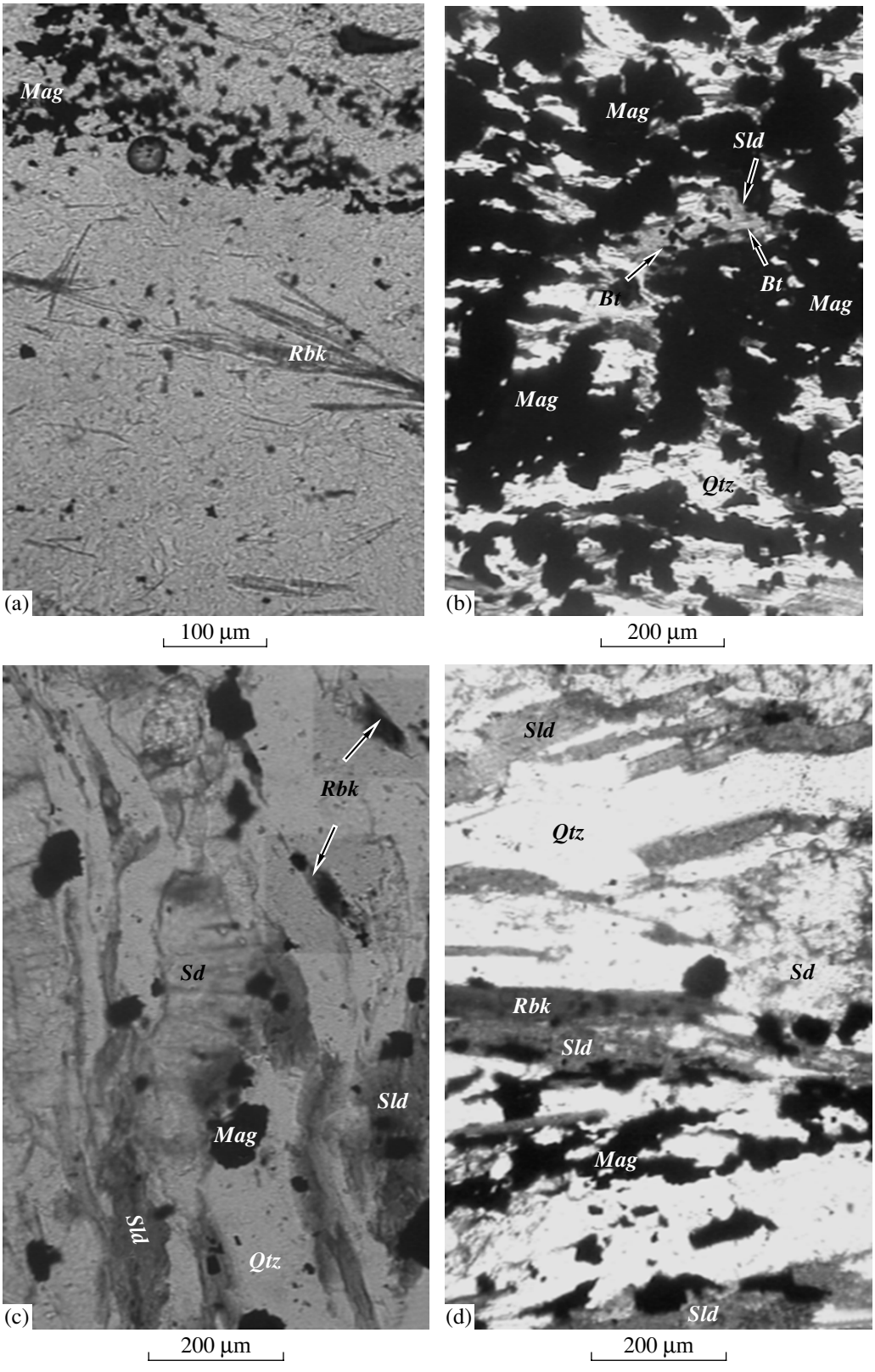

Fig. 4. Micrographs of reaction textures in BIF from the Mikhailovskoe iron deposit.
(a) Acicular riebeckite crystals develop in a quartz–magnetite matrix, sample 467r/214; (b) tetraferribiotite (light gray) is replaced by celadonite (dark gray) in the margins in a magnetite layer, sample 3830/21; (c) celadonite and riebeckite replace siderite, sample 3830/28; (d) celadonite is replaced by riebeckite, sample 3830/28. All micrographs were taken with one polarizer.

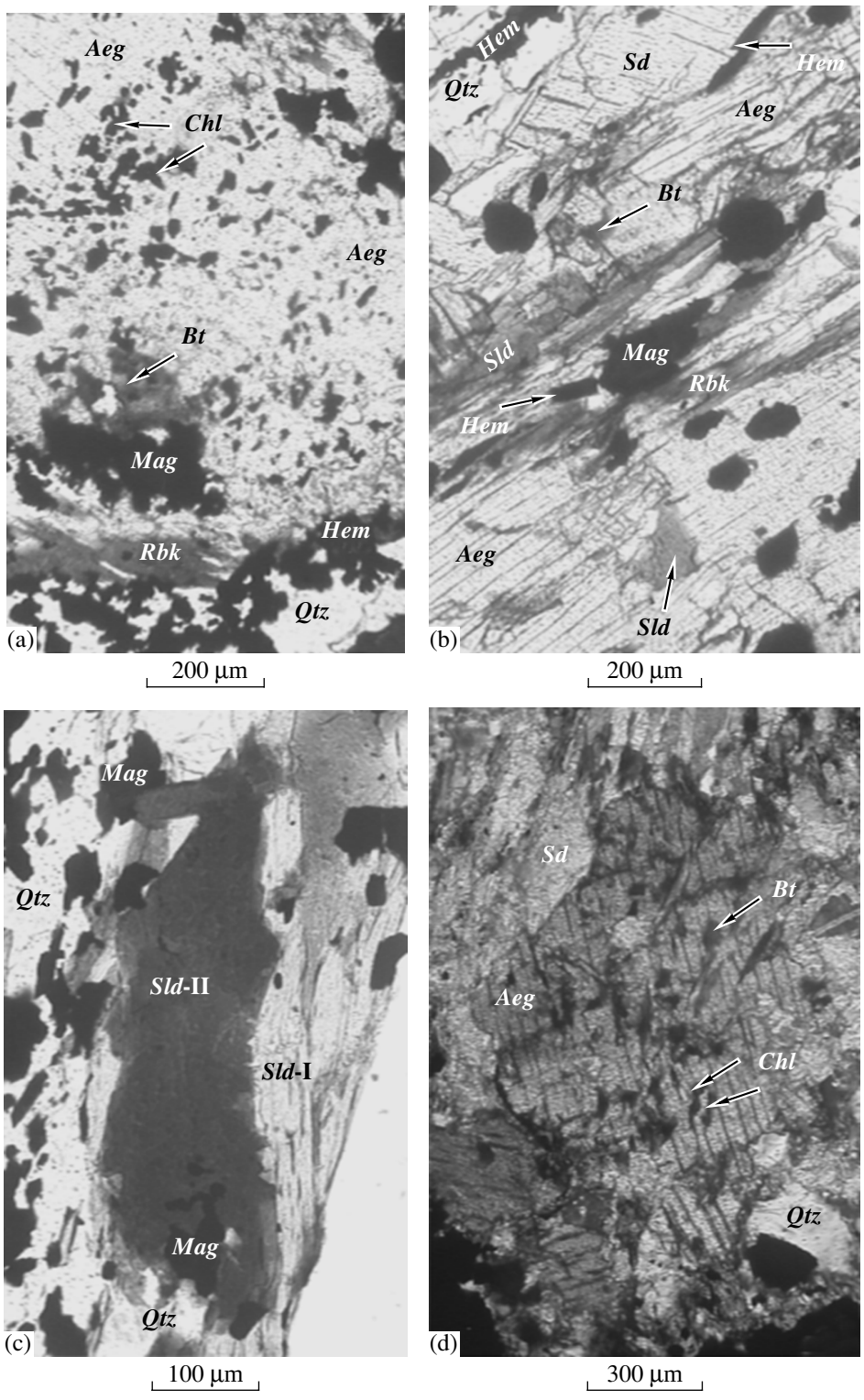

Fig. 5. Micrographs of reaction textures in BIF from the Mikhailovskoe iron deposit.

(a) Large aegirine grain with tetraferribiotite, chlorite, and magnetite inclusions; aegirine is replaced by retrograde riebeckite in the margins, sample 3830/29. (b) Siderite is replaced by aegirine, the latter contains celadonite inclusions and is replaced by retrograde riebeckite along cracks, sample 3830/40. (c) Two populations of celadonite, sample 3830/49. (d) Large aegirine crystals grow in carbonate domains, the aegirine contains tetraferribiotite and chlorite inclusions, sample 3829/7 (one polarizer). (e) Riebeckite develops in celadonite layers, sample 466r/100.

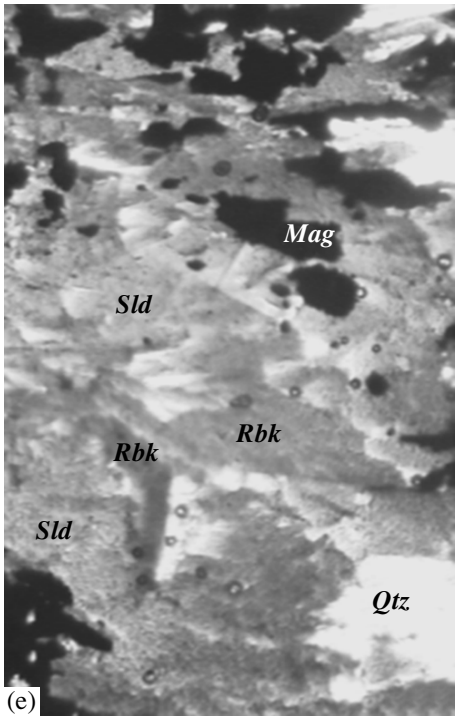

Fig. 5. (Contd.)

close to that of the end member of the annite–ferriannite series and shift toward tetraferriphlogopite in the tetraferriannite–tetraferriphlogopite series (Fig. 7). The KMA tetraferribiotite is also noted for an elevated MnO concentration (up to 0.66 wt %) as compared with those in ferriannite from other iron formations (which contains no more than 0.1 wt %).

The iron formations at the Mikhailovskii prospect of KMA usually contain another green mica, whose composition corresponds to *celadonite*, having the formula $KFe^{3+}(Mg, Fe^{2+})\square[Si_4O_{10}](OH)_2$ (Rieder *et al.*, 1999).

Dioctahedral micas were first studied in the KMA BIF in the 1950–1960s (Sudovikova, 1956; Illarionov, 1965; Foster, 1959). E.N. Sudovikova described a green mica in the KMA BIF in 1956. The mica was in assemblage with aegirine and alkaline amphibole. Mega- and microscopic research led her to ascribe this mica to the phlogopite–lepidomelane series. Later M. Foster (1959) arrived at the conclusion that the green mica from the KMA BIF is not trioctahedral, because its crystal chemical formula appeared to be close to that of dioctahedral potassic mica celadonite.

Celadonite is present in most of our samples, occurring as flakes of emerald green color, ranging from a few tenths of a millimeter to 1.5–2 mm, whose amount sometimes attains 30–40 modal % (Figs. 4d, 5e, 6b–6d).

Celadonite occurs in interlaced aggregates with riebeckite (Fig. 5e), and their crystals (platelets and tables; Fig. 6d, 6e) in magnetite layers are larger than in quartz layers. Aggregates of celadonite and riebeckite can develop as rims around large carbonate grains and separate them from the granoblastic quartz aggregate. Riebeckite sometimes pseudomorphs celadonite (Fig. 4d), or tiny riebeckite needles ("nuclei") occur between magnetite and celadonite grains. Celadonite flakes often develop after carbonate (Fig. 4c). Carbonate domains and the quartz matrix are separated by magnetite–celadonite intergrowths.

The celadonite is very low in Al, has a relatively high X_{Fe} (equal to 0.27–0.41; Table 5), and approaches ferroceladonite of the celadonite–ferroceladonite series (Fig. 8).

The celadonite can be subdivided into two textural groups (Fig. 5c). Celadonite in association with aegirine is usually anhedral, cloud-shaped, while this mineral in the absence of aegirine is mostly platy. Anhedral celadonite develops in cleavage fractures of the platy celadonite. Optically, the platy and anhedral celadonites are also different: when platy, this minerals is pleochroic from dark green to pale yellow or greenish yellow, while the anhedral celadonite, composing irregularly shaped aggregates without visible cleavage, is pleochroic from emerald green to green. The two types of celadonite have practically identical compositions.

Chlorite develops as small (no more than 0.5 mm) reddish brown crystals, which were found exclusively in hematite–magnetite layers free of carbonates or as inclusions, together with magnetite, in aegirine. In the latter situation, chlorite inclusions are restricted to the marginal portions of aegirine crystals, whereas chlorite is absent at aegirine contacts with hematite and from the groundmass (Figs. 5a, 5d, 6a).

Chlorite in the Mikhailovskoe BIF is usually practically free of Al_2O_3 (<0.5 wt %) and is high in Fe^{3+} (Table 4), with X_{Fe} = 0.54–0.67. Hence, the chlorite composition corresponds to ferrichamosite, a hypothetical end member of the chamosite–ferrichamosite series and a member of the ferriclinochlore–ferrichamosite series (Burt, 1989).

Riebeckite occurs in two morphological types. Type I composes elongated prismatic crystals up to 2–5 mm long, of bluish green color with noticeable pleochroism from greenish gray to bluish green and bluish yellow, composing layers of bright blue color up to 1 cm thick (Fig. 6c). The other morphological type of riebeckite comprises acicular aggregates and sheaves of bluish crystals or chains of dark blue crystals 0.5–1 mm long (Fig. 4a) pleochroic from colorless to dark blue.

Riebeckite develops as pseudomorphs after celadonite and tetraferribiotite (Figs. 4d, 5e) and is usually restricted to magnetite layers or carbonate domains. It is also common as inclusions in aegirine and, in these rocks, is absent from their groundmass. Finely acicular riebeckite can replace aegirine along cleavage planes (Figs. 5a, 5b).

Riebeckite in the Mikhailovskoe BIF is fairly magnesian (X_{Fe} = 0.36–0.66, Table 6) and, except for three

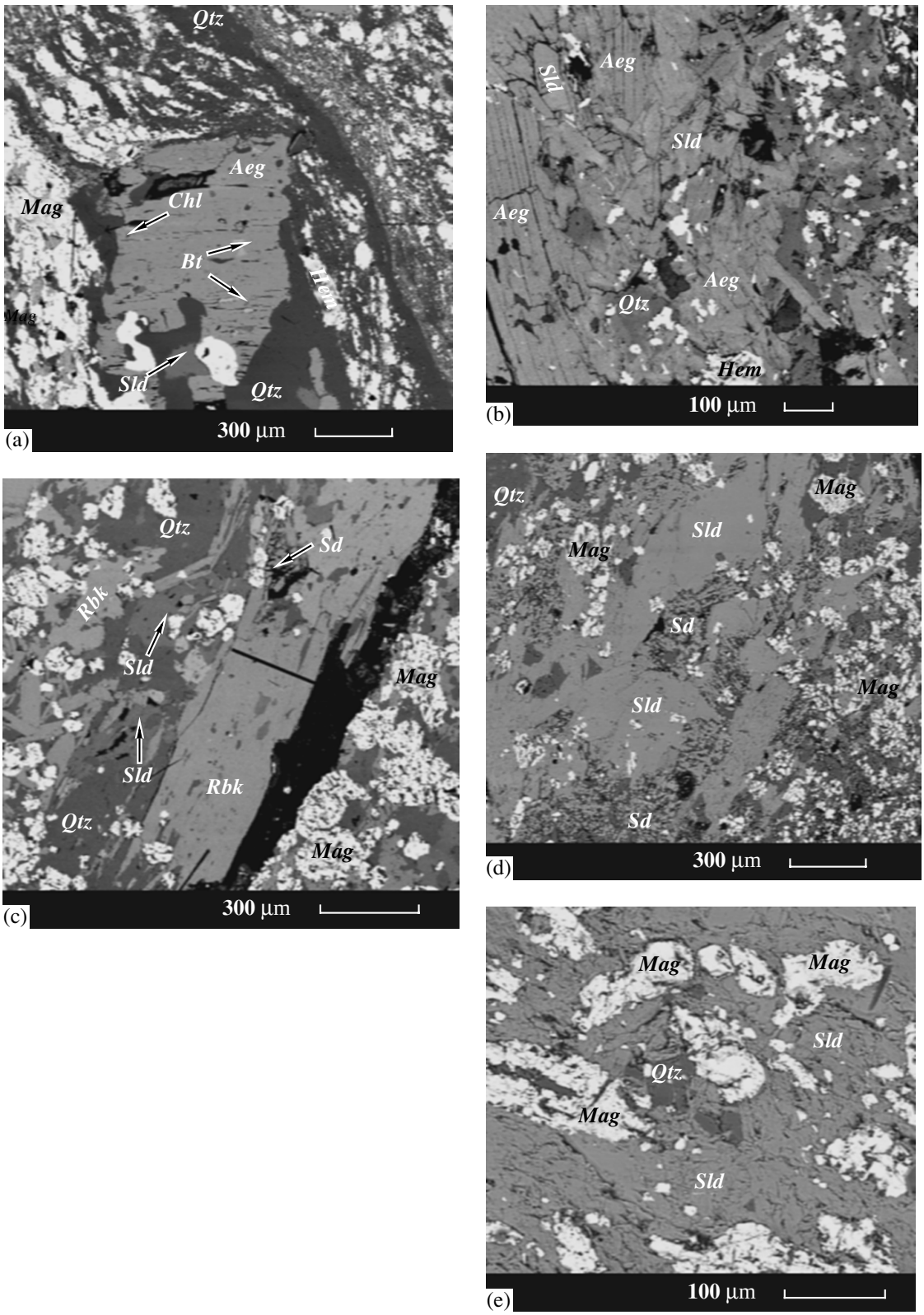

Fig. 6. BSE images of thin sections of BIF from the Mikhailovskoe iron deposit.

(a) Large aegirine grain with tetraferribiotite and chlorite inclusions, sample 3213/8. (b) Intergrowths of celadonite with aegirine, sample 3830/14. (c) Large riebeckite crystal with siderite inclusions, sample 3830/58. (d) Celadonite grows in a quartz–magnetite matrix, sample 460r/86. (e) Celadonite layer in BIF; celadonite develops at the sacrifice of quartz and magnetite.

Table 4. Chemical composition of tetraferribiotite, chlorite, and microcline in BIF from the Mikhailovskoe deposit

Component	3213/8			3291/479.0						3213/8			
	incl. in *Aeg*			matrix						incl. in *Aeg*	matrix		
	Chl-32	*Chl*-34	*Chl*-42	*Bt*-1	*Bt*-2	*Bt*-3	*Bt*-8	*Kfs*-5	*Kfs*-7	*Bt*-20	*Bt*-21	*Bt*-23	*Bt*-25
SiO_2	25.18	24.73	24.39	38.48	37.52	38.26	37.61	63.99	64.09	37.46	37.65	36.92	38.66
TiO_2	0.02	0.02	–	0.37	0.43	0.35	0.40	–	0.03	0.01	–	–	0.04
Al_2O_3	0.24	0.20	0.42	0.71	0.68	0.68	0.76	16.02	16.46	0.53	0.88	1.12	2.60
FeO	51.47	49.45	47.31	31.61	31.49	30.13	32.18	3.01	2.74	37.13	38.43	43.70	29.60
MnO	0.05	–	0.07	0.66	0.51	0.50	0.66	–	0.05	0.23	0.15	0.01	0.12
MgO	9.02	9.61	12.53	14.09	12.69	13.69	12.53	–	–	10.86	10.13	4.45	12.43
CaO	0.18	0.12	0.11	0.02	–	0.11	–	0.03	0.01	0.50	0.20	0.02	0.25
Na_2O	0.03	0.01	0.03	0.02	0.01	0.05	0.03	0.09	–	0.06	0.15	–	0.04
K_2O	0.11	0.12	0.12	9.35	8.98	8.68	9.26	16.84	16.58	7.59	8.11	7.35	8.90
F	n.a.	n.a.	n.a.	0.24	0.03	0.10	0.23	n.a.	n.a.	n.a.	n.a.	n.a.	n.a.
Cl	n.a.	n.a.	n.a.	0.03	0.03	0.05	0.01	n.a.	n.a.	n.a.	n.a.	n.a.	n.a.
Total	86.30	84.26	84.98	95.48	92.37	92.60	93.67	99.99	99.95	94.37	95.70	93.57	92.64
	14O			11O				8O		11O			
Si	3.06	3.06	2.93	3.09	3.14	3.17	3.11	2.99	2.99	3.13	3.11	3.25	3.20
Ti	–	–	–	0.02	0.03	0.02	0.02	–	–	–	–	–	–
Al(IV)	0.04	0.03	0.06	0.07	0.07	0.07	0.07	0.88	0.91	0.05	0.09	0.12	0.25
Fe^{3+}	1.87	1.88	2.12	0.84	0.79	0.76	0.82	0.12	0.11	0.82	0.80	0.63	0.55
Fe^{2+}	3.35	3.23	2.62	1.45	1.63	1.61	1.58	–	–	1.82	1.85	2.59	1.49
Mn	0.01	–	0.01	0.04	0.04	0.04	0.05	–	–	0.02	0.01	–	0.01
Mg	1.63	1.77	2.24	1.69	1.58	1.69	1.54	–	–	1.35	1.25	0.58	1.53
Ca	0.03	0.02	0.02	–	–	0.01	–	–	–	0.04	0.02	–	0.02
Na	0.01	–	0.01	–	–	0.01	–	0.01	–	0.01	0.02	–	0.01
K	0.02	0.02	0.02	0.96	0.96	0.92	0.98	1.00	0.99	0.81	0.85	0.83	0.94
F	–	–	–	0.06	0.01	0.03	0.06	–	–	–	–	–	–
Cl	–	–	–	–	–	0.01	–	–	–	–	–	–	–
X_{Fe}	0.67	0.65	0.54	0.46	0.51	0.49	0.51			0.57	0.60	0.81	0.49

analyses, corresponds to magnesioriebeckite in the classification of Leake *et al.* (1997) (Fig. 9). The MgO concentration ranges within 4.46–9.03 wt %, which is higher than that of riebeckite from other iron formations. For example, according to Robinson *et al.* (1982), this mineral from iron formations contains 1.37–7.71 wt %, although magnesioriebeckite was found in the iron formation of southwestern Labrador (MgO = 17.0 wt %; Klein, 1966).

Aegirine in the iron formation of the Mikhailovskii district forms prismatic crystals 3–4 mm long, which compose layers of grass green color 1–2 cm thick (up to 4 cm in swells) in BIF (Figs. 3, 5a). Aegirine crystals sometimes develop as masses of sheaf-shaped aggregates (Fig. 6b).

Aegirine crystallizes in magnetite and carbonate layers (Fig. 6a). This mineral is rarely accompanied by riebeckite, and, in this situation, riebeckite usually replaces aegirine in the margins and along cracks (Figs. 5a, 5b). The aegirine contains inclusions of chlorite, celadonite, riebeckite, and tetraferribiotite (Figs. 5a, 5b, 5d, 6a). Most samples with aegirine from metalliferous layers contain hematite.

The aegirine is low in Al_2O_3 (0.02–0.12 wt %), TiO_2 (no more than 0.10 wt %), CaO (0.02–0.31 wt %), MgO (no more than 0.17 wt %), and MnO (no more than 0.21 wt %) (Table 7) and corresponds to the end member of the aegirine–augite series.

Carbonates of the iron formation at the Mikhailovskoe deposit composes layers up to 1–2 cm thick and lenses and domains of nearly oval shape. The carbonates develop as equant or elongated grains 0.2–0.7 mm and belong to the ankerite–ferrodolomite series or are dolomite (Table 3). Carbonates of the ferrodolo-

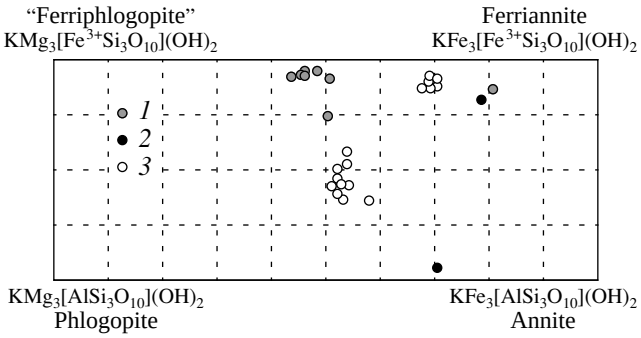

Fig. 7. Compositions of tetraferribiotite shown in a classification plot.
Rocks containing tetraferribiotite: (*1*) BIF from the Mikhailovskoe deposit; (*2*) Penge iron formation, South Africa; (*3*) Dales George, West Australia.

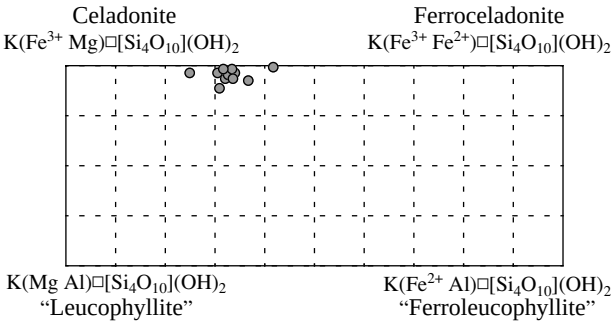

Fig. 8. Compositions of celadonite shown in a classification plot.

mite–ankerite series have Fe/(Fe + Mg) = 0.29–0.59, with most of the values ranging from 0.32 to 0.37. The siderite is more ferrous: Fe/(Fe + Mg) = 0.53–0.67. Siderite is common in oxidized varieties of BIF, and ankerite and dolomite are usually accompanied by magnetite, celadonite, riebeckite, and aegirine (Figs. 4c, 4d, 5b). Siderite inclusions are sometimes contained in large riebeckite crystals (Fig. 6c). The siderite and ankerite contain minor MgO admixtures, up to 1.24 wt % (Table 3).

Potassic feldspar (microcline) is a very rare mineral and was found only in four samples in association

Table 5. Chemical composition of celadonite in BIF from the Mikhailovskoe deposit

Component	466p/131.0		469p/254.0		460p/86			MK-1	
	2	3	1	3	1	2	3	1	2
SiO_2	50.49	50.85	51.58	51.15	50.79	50.97	50.72	51.09	51.72
TiO_2	0.01	0.01	–	–	0.01	–	0.01	0.01	–
Al_2O_3	0.49	0.35	0.49	0.12	0.54	0.84	1.35	0.12	0.49
FeO	26.15	26.07	25.80	26.01	25.67	26.73	26.32	26.67	25.68
MnO	–	–	–	0.01	0.02	0.01	–	0.02	0.01
MgO	4.80	4.90	4.68	4.59	5.02	4.54	4.34	4.62	4.58
CaO	0.05	0.01	–	–	0.01	0.02	0.01	0.01	0.02
Na_2O	0.05	0.04	–	0.06	–	0.02	0.02	–	0.02
K_2O	10.66	10.35	10.64	10.24	10.54	10.90	10.82	10.80	10.84
Total	92.70	92.58	93.19	92.18	92.60	94.03	93.59	93.34	93.36
				11O					
Si	3.77	3.80	3.83	3.85	3.79	3.76	3.75	3.80	3.83
Ti	–	–	–	–	–	–	–	–	–
Al(VI)	0.04	0.03	0.04	0.01	0.05	0.07	0.12	0.01	0.04
Fe^{3+}	1.44	1.36	1.30	1.28	1.37	1.44	1.40	1.42	1.32
Fe^{2+}	0.19	0.27	0.30	0.35	0.22	0.20	0.23	0.24	0.27
Mn	–	–	–	–	–	–	–	–	–
Mg	0.53	0.55	0.52	0.51	0.56	0.50	0.48	0.51	0.51
Ca	–	–	–	–	–	–	–	–	–
Na	0.01	0.01	–	0.01	–	–	–	–	–
K	1.01	0.99	1.01	0.98	1.00	1.02	1.02	1.02	1.02
X_{Fe}	0.27	0.33	0.37	0.41	0.29	0.29	0.32	0.32	0.35

Table 6. Chemical composition of riebeckite in BIF from the Mikhailovskoe deposit

Component	MK-2				3830/58							3195/15			
	incl. in *Aeg*		matrix		profile across a large riebeckite crystal						matrix	matrix			
	41	43	45	48	margin	→	core	→	→	margin	9	61	63	67	69
SiO_2	52.70	52.24	52.49	52.71	54.31	53.17	54.26	54.15	53.79	53.85	53.90	53.56	54.26	53.66	54.20
TiO_2	–	–	0.01	0.01	0.01	–	0.05	–	0.06	–	–	0.36		0.03	0.05
Al_2O_3	0.01	0.04	0.02	–	0.53	0.09	0.16	0.68	0.61	0.53	0.51	–	0.71	0.06	0.17
FeO	31.02	30.85	33.65	31.28	28.02	27.06	26.19	27.53	28.08	28.23	27.58	27.93	26.61	28.82	26.94
MnO	0.01	0.01	–	0.05	–	–	–	–	–	–	0.11	0.09	–	–	0.04
MgO	6.32	6.61	4.46	6.06	7.91	8.72	9.03	8.17	7.66	7.85	7.99	8.01	8.67	7.29	8.76
CaO	0.12	0.03	0.02	0.09	0.04	0.09	0.12	0.17	0.14	0.04	0.15	0.01	0.07	0.05	0.13
Na_2O	6.79	6.90	6.93	7.02	6.97	7.65	7.60	7.30	7.56	7.3	7.69	7.41	7.29	7.53	7.33
K_2O	0.23	0.40	0.13	0.18	–	0.22	0.60	–	–	–	0.09	0.03	0.09	0.26	0.39
Total	97.20	97.08	97.71	97.40	97.79	97.00	98.01	98.00	97.90	97.80	98.02	97.49	97.70	97.70	98.01
							23O								
Si	7.78	7.73	7.82	7.80	7.83	7.78	7.85	7.81	7.82	7.80	7.83	7.81	7.82	7.87	7.83
Ti	–	–	–	–	–	–	0.01	–	0.01	–	–	0.04	–	–	0.01
Al	–	0.01	–	–	0.09	0.02	0.03	0.12	0.10	0.09	0.09	–	0.12	0.01	0.03
Fe^{3+}	2.41	2.48	2.32	2.33	2.28	2.19	1.97	2.17	2.07	2.25	2.03	2.17	2.17	2.05	2.14
Fe^{2+}	1.41	1.33	1.86	1.53	1.10	1.12	1.19	1.15	1.34	1.17	1.31	1.23	1.03	1.48	1.11
Mn	–	–	–	0.01	–	–	–	–	–	–	0.01	0.01	–	–	–
Mg	1.39	1.46	0.99	1.34	1.70	1.90	1.95	1.76	1.66	1.69	1.73	1.74	1.86	1.59	1.88
Ca	0.02	–	–	0.01	0.01	0.01	0.02	0.03	0.02	0.01	0.02	0.02	0.01	0.01	0.02
Na	1.94	1.98	2.00	2.01	1.95	2.17	2.13	2.04	2.13	2.05	2.16	2.09	2.03	2.14	2.05
K	0.04	–	0.02	0.03	–	0.04	0.11	–	–	–	0.02	0.01	0.02	0.05	0.07
X_{Fe}	0.51	0.48	0.66	0.54	0.39	0.37	0.38	0.40	0.45	0.41	0.43	0.41	0.36	0.48	0.37

with tetraferribiotite and celadonite. It is greenish (owing to the presence of Fe^{3+} in amounts of 2.74–3.01 wt %), which substitutes Al^{3+} at the T site (Table 4). This composition of the microcline was caused by the chemistry of the rock, namely, its richness in Fe^{3+} and a low alumina content.

Some rocks contain accessory apatite.

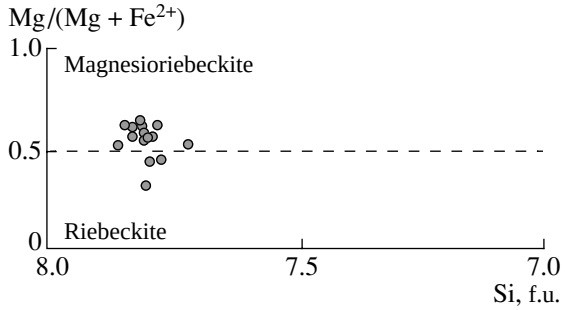

Fig. 9. Compositions of riebeckite from the Mikhailovskoe BIF shown in a classification plot.

METAMORPHIC *P–T* PARAMETERS

The rocks of the iron formation contain no minerals traditionally used as geothermometers and geobarometers. Moreover, there are no consistent thermodynamic data on many minerals of these rocks. Because of this, most researchers utilize thermobarometric estimates for the rocks hosting BIF, most often, metapelites. Earlier, in studying mineral equilibria in the chloritoid schists underlying BIF of the Stoilenskaya Formation, Kurskaya Group in the Mikhailovskii district, the following mineral assemblages were described: *Qtz* + *Cld* + *Chl*, *Qtz* + *Cld* + *Chl* + *Ms*, *Qtz* + *Cld* + *Chl* + *Ms* + *And*, and *Qtz* + *Cld* + *Grt* + *Chl* + *Ms* + *Bt* in the almandine–chlorite–chloritoid zone and *Qtz* + *St* + *Cld* + *Chl* + *Ms*, *Qtz* + *St* + *And* + *Cld* + *Chl* + *Bt* in the chloritoid–staurolite zone (Poskryakova, 2001). The appearance of staurolite in association with chloritoid in metapelites testifies for the transition from the almandine–chlorite–chloritoid zone of the greenschist facies to the staurolite–chlorite–chloritoid zone of the staurolite facies (Korikovsky, 1979). The *St* + *Cld* + *Bt* assemblage is stable over the temperature interval of 450–520°C at pressures of 2–3 kbar, according to the petrogenetic grid in (Spear and Cheney, 1989). Stauro-

Table 7. Chemical composition of aegirine in BIF from the Mikhailovskoe deposit

Component	3213/8	MK-18					3830/14			3195/15				
	29	21	22	23	28	31	47	48	50	60	62	64	66	70
	margin	margin	core	margin	core	margin	margin	core	margin	margin	margin	margin	core	margin
SiO_2	53.21	52.89	52.79	53.09	53.29	53.05	52.77	52.75	53.37	53.09	53.02	53.58	52.92	53.34
TiO_2	–	0.10	–	–	–	–	0.10	–	0.02	0.03	0.02	0.12	0.04	0.02
Al_2O_3	0.02	0.23	0.06	0.11	0.11	0.09	0.14	0.21	0.15	0.09	0.17	0.10	0.21	0.05
FeO	32.57	32.90	31.82	32.11	32.52	32.95	31.47	32.23	32.67	31.69	32.13	32.20	32.72	32.97
MnO	–	0.21	0.04	–	0.02	–	0.15	–	0.13	–	0.14	–	–	–
MgO	0.02	0.14	0.04	0.02	0.05	–	0.03	–	–	–	0.07	0.17	0.04	–
CaO	0.14	0.15	0.18	0.08	0.05	0.19	0.19	0.31	0.02	0.23	0.19	0.23	0.31	0.19
Na_2O	13.21	13.34	15.01	14.42	13.95	13.65	15.00	14.37	13.62	14.80	14.26	13.55	13.63	13.37
K_2O	–	–	0.05	–	–	0.03	0.01	0.07	0.01	0.05	0.03	–	0.01	0.03
Total	99.17	99.96	99.99	99.83	99.99	100.00	99.86	99.94	99.99	99.98	100.03	99.95	99.98	99.97
Si	2.00	1.98	1.94	1.96	1.98	1.98	1.94	1.95	1.99	1.95	1.96	1.99	1.97	1.99
Ti	–	–	–	–	–	–	–	–	–	–	–	–	–	–
Al	–	0.01	–	–	–	–	0.01	0.01	0.01	–	0.01	–	0.01	–
Fe^{3+}	0.95	1.00	1.19	1.10	1.04	1.03	1.18	1.12	1.00	1.14	1.09	0.97	1.03	0.98
Fe^{2+}	0.07	0.03	–	–	–	–	–	–	0.02	–	–	0.03	–	0.05
Mn	–	0.01	–	–	–	–	–	–	–	–	–	–	–	–
Mg	–	0.01	–	–	–	–	–	–	–	–	–	0.01	–	–
Ca	0.01	0.01	0.01	–	–	0.01	0.01	0.01	–	0.01	0.01	0.01	0.01	0.01
Na	0.96	0.97	1.07	1.03	1.00	0.99	1.07	1.03	0.98	1.06	1.02	0.98	0.98	0.97
K	–	–	–	–	–	–	–	–	–	–	–	–	–	–

lite-free assemblages with chloritoid, chlorite, and muscovite are stable at 370–470°C within the andalusite stability field. It follows that the prograde *P–T* metamorphic path, inferred from the phase equilibria and mineralogical thermometric data, can be estimated at 370–520°C at 2–3 kbar.

PETROGENESIS

The wide occurrence of K- and Na-bearing minerals in rocks of the iron formation in the Mikhailovskii district suggests that the protoliths of these rocks were the products of sedimentation and diagenesis of iron–silicate gels rich in Na and K (French, 1973; Klein, 1974). When this material starts to crystallize during diagenesis, the diffusion of cations is activated, and Na and K can be accommodated in the structures of mica and riebeckite. Eugster (1969) suggested, by analogy with Pleistocene siliceous lacustrine deposits, that magadiite $NaSi_7O_{13} \cdot 3H_2O$ was the first to crystallize in the iron-formation deposits. As a consequence of reaction with Fe-bearing mixed-layer silicates, Na was released and gave rise to riebeckite (Miyano, 1982). The very low-temperature metamorphism produced disordered K-micas almost devoid of Al, and their decomposition resulted in celadonite and tetraferribiotite.

Conceivably, part of the riebeckite, celadonite, and tetraferribiotite could crystallize from alkali-bearing solutions that entered the rocks during their deformations. In the Early Proterozoic iron formation of KMA, limited alkaline metasomatism proceeded within zones permeable to fluid (such as zones of fracturing and intense tectonization). This is confirmed by the observations of Trendall and Blockley (1970) that riebeckite develops in the iron formations of western Australia in close relation with deformations. Glagolev (1966) noted that the activity of alkaline metasomatism in the KMA iron formation was generally not high. The BIF with aegirine and riebeckite fully preserved their characteristic structures (thin banding and crenulation) and bear no metasomatic bodies with massive or impregnated structures. The aegirine and riebeckite coexist with quartz, magnetite, hematite, micas, and carbonates, i.e., there are absolutely no monomineralic and bimineralic associations. Because of this, Glagolev (1966) referred to the limited alkaline metasomatism in BIF as alkaline metamorphism.

The stability of hematite and magnetite in the BIF mineral assemblages testifies to high values of oxygen

fugacity, close to the magnetite–hematite buffer. This is corroborated by the elevated X_{Mg} of the tetraferribiotite, celadonite, chlorite, and riebeckite, because, in the general case, the X_{Fe} of Fe–Mg silicates decreases with increasing oxygen fugacity. An elevated oxygen fugacity during the metamorphism and the low Al_2O_3 concentration in the rocks account for the fact that the Mikhailovskoe BIF contain minerals high in Fe^{3+}. For example, these rocks ubiquitously bear celadonite and tetraferribiotite, which seem to have been stable throughout the whole greenschist facies. Low-temperature iron formations elsewhere commonly contain stilpnomelane (Klein and Gole, 1981; Haase, 1982; Floran and Papike, 1978; and others). Although the metamorphic parameters of the Mikhailovskoe BIF are above the stability field of this mineral (approximately 470°C at 2–3 kbar; Miyano and Klein, 1989), the latter was likely not stable even at lower temperatures because of the low alumina concentrations in the rocks and their high Fe_2O_3/FeO ratios. This is confirmed by the absolute absence of grunerite, which is, along with other minerals, an inevitable product of stilpnomelane decomposition at low pressures (Miyano and Klein, 1989). In place of stilpnomelane, the rocks contain widespread tetraferribiotite and celadonite, which suggests an elevated K^+ activity in the fluid.

Instead of greenalite $Fe_6Si_4O_{10}(OH)_8$, a mineral common in BIF of low metamorphic grades, the Mikhailovskoe rocks contain its "oxidized" analogue ferrichamosite (Fe^{2+}_5 $Fe^{3+}[Fe^{3+}Si_3O_{10}](OH)_8$. Chlorites are generally rare in iron formations because of the low Al_2O_3 contents of the rocks (Laird, 1989) and are commonly represented by chamosite (Gole, 1980) and, more rarely, clinochlore and ripidolite (Klein, 1983; Miyano and Beukes, 1997), which crystallize at the lowest metamorphic grades and, perhaps, catagenesis.

MINERAL FACIES

The reaction texture, described above, of alkali-rich BIF at the Mikhailovskoe deposit can be interpreted with the aid of chemical reactions in the system Na_2O–K_2O–FeO–Fe_2O_3–SiO_2–CO_2–H_2O.

The replacement textures of tetraferribiotite by celadonite suggest the oxidation of the former according to the reaction

$$\begin{gathered} Bt + Qtz + 1/2O_2 \longrightarrow Sld + Hem \\ K(Fe^{2+}, Fe^{3+})_3[Fe^{3+}Si_3O_{10}](OH)_2 + SiO_2 \\ + 1/2O_2 \longrightarrow KFe^{3+}Fe^{2+}[Si_4O_{10}](OH)_2 + Fe_2O_3 \end{gathered} \quad (1)$$

or

$$\begin{gathered} Bt + Qtz + 1/3O_2 \longrightarrow Sld + 2/3Mag \\ K(Fe^{2+}, Fe^{3+})_3[Fe^{3+}Si_3O_{10}](OH)_2 + SiO_2 \\ + 1/3O_2 \longrightarrow KFe^{3+}Fe^{2+}[Si_4O_{10}](OH)_2 + 2/3Fe_3O_4, \end{gathered} \quad (2)$$

and, depending on the oxygen fugacity in discrete layers, hematite [at higher f_{O_2}, reaction (1)] or magnetite [at lower f_{O_2}, reaction (2)] are formed in the right-hand sides of the reactions.

Aegirine and riebeckite were never found in equilibrium relations and generally occur simultaneously very rarely. They usually compose discrete layers, which, however, can be not far from one another. Even if the two minerals occur in the same layer, riebeckite retrogressively replaces aegirine grains in margins and along cracks or is contained as inclusions in aegirine. Hematite in most rocks coexists with riebeckite in aegirine-free layers but can also be absent from them. Hence, the stability of aegirine or riebeckite in the iron formations is more probably controlled by the oxygen fugacity rather than the temperature of metamorphism

$$\begin{gathered} 4Rbk + 3O_2 \longrightarrow 8Aeg + 6Hem + 16Qtz + H_2O \\ 4Na_2(Fe^{3+}Fe^{2+})_5[Si_8O_{22}](OH)_2 + 3O_2 \\ \longrightarrow 8NaFe^{3+}[Si_2O_6] + 6Fe^{3+}_2O_3 + 16SiO_2 + 4H_2O. \end{gathered} \quad (3)$$

REGIME OF OXYGEN AND ALKALIS DURING METAMORPHISM

Riebeckite presence in iron formations is controlled by f_{O_2}, a_{Na^+}, and temperature (Miyano and Klein, 1983). Furthermore, if riebeckite occurs in assemblage with ankerite and/or siderite, its stability field expands with the increasing CO_2 activity in the fluid. The stability of riebeckite in iron formations cannot serve as an clear-cut indicator of the metamorphic temperature interval if other factors are not accounted for. Riebeckite (more specifically, its asbestiform variety crocidolite) can develop at the sacrifice of iron oxides, carbonates, and quartz at very low temperature metamorphism or even diagenesis, starting from 130°C, at the active interaction of Fe-rich rocks with Na^+-bearing solutions (Miyano and Klein, 1983).

Since aegirine and riebeckite rarely occur together in our rocks and compose different layers at the Mikhailovskoe deposit, it is reasonable to conclude that no reaction of high-temperature riebeckite decomposition with the origin of aegirine *Rbk* + *Hem* = *Aeg* + *Mag* + *Qtz* + H_2O took place. This makes it possible to constrain the upper temperature boundary of metamorphism. The position of reaction lines in the diagram was constrained experimentally (Ernst, 1962) and calculated (Miyano and Beukes, 1997). According to these data, high-temperature riebeckite decomposition with the origin of aegirine proceeds at 510–520°C, 2.5 kbar, and a_{H_2O} = 1.0 and is independent of oxygen fugacity and sodium activity in the fluid.

Our BIF never contain grunerite, but reaction relationships between grunerite and riebeckite were described in the Penge iron formation, South Africa,

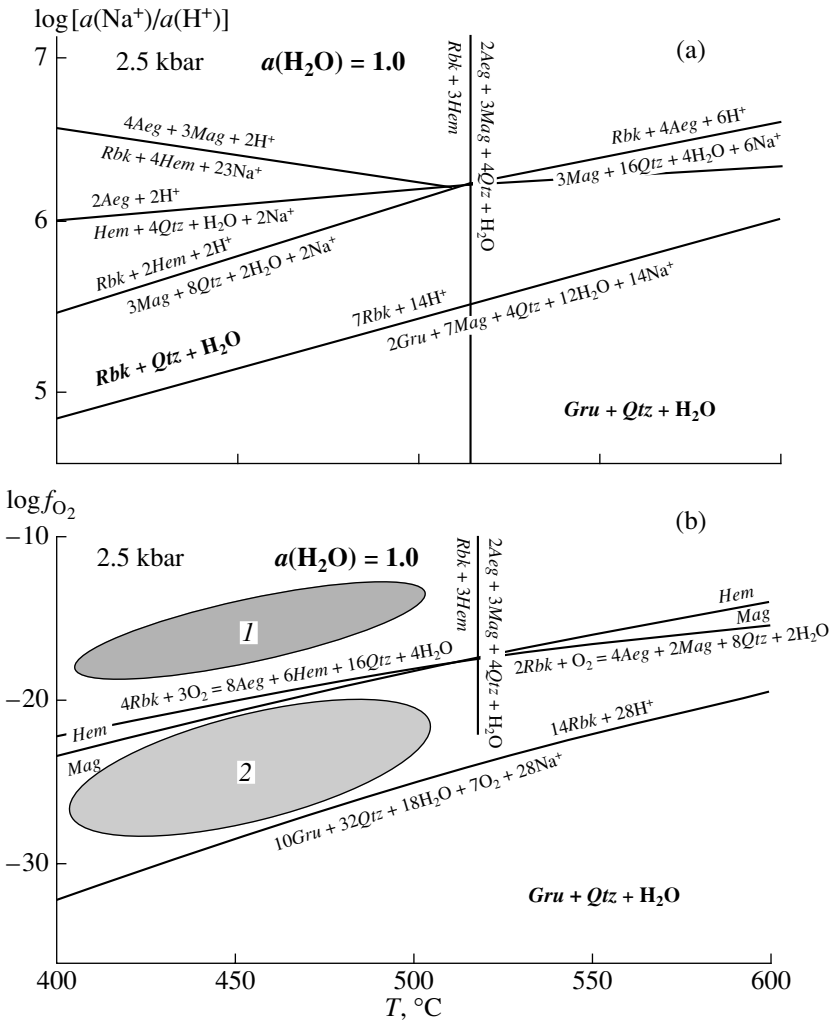

Fig. 10. Stability of riebeckite shown in (a) $[\log[a(Na^+)/a(H^+)]$ vs. *T* and (b) $\log[f_{O_2}]$ vs. *T* diagrams. Shaded fields correspond to: (*1*) stability of the *Rbk* + *Mag* assemblage and (*2*) stability of the *Aeg* + *Hem* assemblage, calculated for a pressure of 2.5 kbar and $a(H_2O) = 1.0$ (according to Miyano and Beukes, 1997).

(Miyano and Beukes, 1997) and the Prioskol'skoe iron deposit of KMA (Savko and Kal'mutskaya, 2002). Miyano and Beukes (1997) calculated the position of the reaction *Gru* + *Mag* + *Qtz* + H_2O = *Rbk* in a $\log[a(Na^+)/a(H^+)]$ vs. *T* as a function of the Na activity in the fluid. According to the data of these researchers, riebeckite is stable instead of grunerite at a high Na activity, $[\log[a(Na^+)/a(H^+) > 5.0–5.5$ over the temperature interval of 400–500°C (Fig. 10). At a higher Na activity, riebeckite should decompose and produce aegirine by the reaction *Rbk* + *Hem* + Na^+ = *Aeg* + *Mag* + H^+, which proceeds at $\log[a(Na^+)/a(H^+) = 6.5$ at 400°C. No such reaction took place in our rocks, because they contain aegirine, but not riebeckite, in association with hematite. Hence, metamorphic transformations of the Mikhailovskoe iron formations occurred at a high Na activity in the fluid at $\log[a(Na^+)/a(H^+)] = 5.0–6.5$ (Fig. 10).

According to Miyano and Beukes (1997), aegirine forms at the expense of riebeckite by the following reactions at different metamorphic regimes:

Rbk + 3*Hem* = 2*Aeg* + 3*Mag* + 4*Qtz* + H_2O if the temperature increases;

2*Rbk* + O_2 = 4*Aeg* + 2*Mag* + 8*Qtz* + $2H_2O$ if the oxygen fugacity increases;

Na^+ – *Rbk* + 4*Hem* + $23Na^+$ = 4*Aeg* + 3*Mag* + $2H^+$ if the sodium activity increases.

The latter reaction producing magnetite and aegirine occurs in the high-temperature region, at temperatures above 510°C (Miyano and Beukes, 1997). It follows that the only plausible mechanism forming aegirine from riebeckite in our BIF is reaction (3): 4*Rbk* + $3O_2 \longrightarrow$ 8*Aeg* + 6*Hem* + 16*Qtz* + $4H_2O$, which is

controlled by the redox conditions of metamorphism. The position of this reaction in a $\log(f_{O_2}) - T\,^\circ C$ space calculated for 2.5 kbar and $a_{H_2O} = 1$ nearly coincides with the hematite–magnetite buffer over the temperature interval of 400–500°C (Miyano and Beukes, 1997). Hence, the occurrence of aegirine or riebeckite in the alkali-rich BIF at KMA is a sensitive indicator of oxygen fugacity during metamorphism (Fig. 10).

In most Precambrian iron formations, oxygen behaves as a locally dependent (inert) component (Frost, 1982; Fonarev, 1987; Savko, 1994). Many researchers admit that oxygen fugacity in metamorphic iron formations depends on its original concentration in them (Korzhinskii, 1940; Marakushev, 1965) and can only little vary during metamorphism because of the inert behavior of this element. In every area or even an individual layer, oxygen fugacity is controlled by the conditions of sedimentation and diagenesis and by buffer reactions. Because of this, oxygen fugacity may vary from layer to layer even within a single iron formation but is thought to remain constant within the layers. This is usually manifested in variations in the X_{Fe} of silicates from layer to layer in the iron formations, for example, these parameters of grunerite and orthopyroxene in the presence of hematite or magnetite. In the alkali-rich iron formations of KMA, the variations in the oxygen fugacity between individual layers are reflected in the stability of the *Aeg + Hem* and *Rbk + Mag* assemblages.

CONCLUSIONS

The early Proterozoic iron formations of the Mikhailovskoe deposit at KMA contain widespread K-bearing, Al-free micas (tetraferribiotite and celadonite), carbonates (ankerite and siderite), riebeckite, and aegirine. Studying the mineral equilibria in the rocks enables reproducing the genetic successions of mineral assemblages and the physicochemical parameters of metamorphism. Early in the course of metamorphic processes, the rocks contained quartz, carbonates, iron oxides, specific K-bearing and Al-free micas, and Fe-rich and Al-free chlorite. Later, depending on the oxygen fugacity in individual layers (above or below the hematite–magnetite buffer), the *Aeg + Hem* or *Rbk + Mag* assemblages developed. The metamorphic temperature is estimated at 370–520°C at pressures of 2–3 kbar, $\log[a(Na^+)/a(H^+)] = 5.5–6.0$, and an oxygen fugacity above the hematite–magnetite buffer in layers containing the *Aeg + Hem* assemblage and below this buffer in layers with the *Rbk + Mag* assemblage.

ACKNOWLEDGMENTS

The authors thank S.P. Korikovsky (Institute of the Geology of Ore Deposits, Petrography, Mineralogy, and Geochemistry, Russian Academy of Sciences) for constructive criticism and valuable comments during the preparation of the manuscript; V.A. Skulkov (Yugozapadgeologiya Geological Survey) and V.N. Babanskii (Mikhailovskii Mining and Processing Enterprise) for help with the fieldwork. This study was financially supported by Russian Universities Grant (project UR.09.01.038), the Russian Foundation for Basic Research (project nos. 03-05-64071, 03-05-79088), President of the Russian Federation (project MD-428.2003.05), and the Integration Federal Program (project E0348).

REFERENCES

Burt, D.M., Vector Representation of Phyllosilicate Compositions, *Rev. Mineral.*, 1989, vol. 19, part 14, pp. 584–599.

Ernst, W.G., Synthesis, Stability Relations, and Occurrence of Ribeckite and Ribeckite–Arfvedsonite Solid Solutions, *J. Geol.*, 1962, vol. 70, pp. 689–736.

Eugster, H.P., Inorganic Bedded Cherts from the Magadi Area, Kenya, *Contrib. Mineral. Petrol.*, 1969, vol. 22, pp. 1–31.

Floran., R.J. and Papike, J.J., Mineralogy and Petrology of the Gunflint Iron Formation, Minnesota–Ontario: Correlation of Compositional and Assemblage Variations at Low to Moderate Grade, *J. Petrol.*, 1978, vol. 19, pp. 215–288.

Fonarev, V.I., *Mineral'nye ravnovesiya zhelezistykh formatsii dokembriya* (Mineral Equilibria in Precambrian BIF), Moscow: Nauka, 1987.

Foster, M.D., Green Mica from BIF of the Kursk Magnetic Anomaly, *Zap. Vses. Mineral. O–va*, 1959, part 88, no. 6, pp. 729–730.

French, B.M., Mineral Assemblages in Diagenetic and Low-Grade Metamorphic Iron Formations, *Econ. Geol.*, 1973, vol. 68, pp. 1063–1074.

Frost, B.R., Contact Metamorphic Effect of the Stillwater Complex, Montana: The Concordant Iron Formation: A Discussion of the Role of Buffering in Metamorphism of Iron Formation, *Am. Mineral.*, 1982, vol. 67, no. 1/2, pp. 142–148.

Glagolev, A.A., *Metamorfizm dokembriiskikh porod KMA* (Metamorphism of the Kursk Magnetic Anomaly Precambrian Rocks), Moscow: Nauka, 1966.

Gole, M.J. and Klein, C., Banded Iron Formation through Much of Precambrian Time, *J. Geol.*, 1981, vol. 89, pp. 169–183.

Gole, M.J., Mineralogy and Petrology of Very Low-Grade Metamorphic Archean Banded Iron Formations, Weld Range, Western Australia, *Am. Mineral.*, 1980, vol. 65, pp. 8–25.

Haase, C.S., Metamorphic Petrology of the Negaunee Iron Formation, Marquette District, Northern Michigan: Mineralogy, Metamorphic Reactions, and Phase Equilibria, *Econ. Geol.*, 1982, vol. 77, pp. 60–81.

Illarionov, A.A., *Petrografiya i mineralogiya zhelezistykh kvartsitov Mikhailovskogo mestorozhdeniya Kurskoi magnitnoi anomalii* (Petrography and Mineralogy of BIF from Mikhailovskoe Deposit, Kursk Magnetic Anomaly), Moscow: Nauka, 1965.

James, H.L., Sedimentary Facies of Iron Formation, *Econom. Geol.*, 1954, vol. 49, pp. 235–285.

Klein, C., Mineralogy and Petrology of the Metamorphosed Wabush Iron Formation, Southwestern Labrador, *J. Petrol.*, 1966, vol. 7, pp. 246–305.

Klein, C., Changes in Mineral Assemblages with Metamorphism of Some Banded Precambrian Iron Formations, *Econ. Geol.*, 1973, vol. 68, pp. 1075–1088.

Klein, C., Greenalite, Minnesotaite, Crocidolite, and Carbonates in a Very Low-Grade Metamorphic Precambrian Iron Formation, *Can. Mineral.*, 1974, vol. 12, pp. 475–498.

Klein, C. and Gole, M.J., Mineralogy and Petrology of Parts of the Marra Mamba Iron Formation, Hamersley Basin, Western Australia, *Am. Mineral.*, 1981, vol. 66, pp. 507–525.

Klein, C., *Diagenesis and Metamorphism of Precambrian Iron Formations*, Trendall, A.F. and Morris, R.C., Eds., Amsterdam: Elsevier, 1983, pp. 417–469.

Korikovsky, S.P., *Fatsii metamorfizma metapelitov* (Facies of Metapelite Metamorphism), Moscow: Nauka, 1979.

Korzhinskii, D.S., *Faktory mineral'nykh ravnovesii i mineralogicheskie fatsii glubinnosti* (Factors of Mineral Equilibria and Mineralogical Facies of Depth), Moscow: Akad. Nauk SSSR, 1940, issue 12, no. 5.

Laird, J., Chlorites: Metamorphic Petrology, *Rev. Miner.*, 1989, vol. 19, Cpt. 11, pp. 405–453.

Leake, B.E., Woolley, A.R., and 20 Members of the Subcommittee on Amphiboles, Nomenclature of Amphiboles. Report of the Subcommittee on Amphiboles of the International Mineralogical Association Commission on New Minerals and Mineral Names, *Eur. J. Miner.*, 1997, vol. 9, pp. 623–651.

Marakushev, A.A., *Problemy mineral'nykh fatsii metamorficheskikh i metasomaticheskikh porod* (Problems of the Mineral Facies of Metamorphic and Metasomatic Rocks), Moscow: Nauka, 1965.

Miyano, T., Stilpnomelane, Fe-Rich Mica, K-Feldspar, and Hornblende in Banded Iron Formation Assemblages of the Dales Gorge Member, Hammersley Group, Western Australia, *Can. Mineral.*, 1982, vol. 20, pp. 189–202.

Miyano, T. and Beukes, N.J., Mineralogy and Petrology of the Contact Metamorphosed Amphibole Asbestos-Bearing Penge Iron Formation, Eastern Transvaal, South Africa, *J. Petrol.*, 1997, vol. 38, no. 5, pp. 651–676.

Miyano, T. and Klein, C., Conditions of Riebeckite Formation in the Iron Formation of the Dales Gorge Member, Hamersley Group, Western Australia, *Am. Mineral.*, 1983, vol. 68, pp. 517–529.

Miyano, T. and Klein, C., Phase Equilibria in the System K_2O–FeO–MgO–Al_2O_3–SiO_2–CO_2–H_2O and the Stability Limit of Stilpnomelane in Metamorphosed Precambrian Iron Formations, *Contrib. Mineral. Petrol.*, 1989, vol. 102, pp. 478–491.

Miyano, T. and Miyano, S., Ferri-Annite from the Dales George Member Iron Formations, Wittenoom Area, Western Australia, *Am. Mineral.*, 1982, vol. 67, pp. 1179–1194.

Poskryakova, M.V., *Fazovye ravnovesiya na granitse zelenoslantsevoi i stavrolitovoi fatsii metamorfizma na primere Mikhailovskogo rudnogo raiona KMA* (Phase Equilibria at the Boundary between the Greenschist and Staurolite Facies of Metamorphism with Reference to the Mikhailovskii Ore Field, Kursk Magnetic Anomaly), *Vestn. Voronezh. Univ., Geologiya*, 2001, issue 11, pp. 122–131.

Rieder, M. *et al.*, Nomenclature of the Micas, *Mineral. Mag.*, 1999, vol. 63(2), pp. 267–279.

Robinson, P., Spear, F.S., *et al.*, Phase Relations of Metamorphic Amphiboles: Natural Occurrence and Theory, *Rev. Mineral.*, 1982, vol. 9, pp. 3–227.

Savko, K.A., Fayalite–Grunerite–Magnetite–Quartz Rocks in BIF of the Voronezh Crystalline Massif: Phase Equilibria and Metamorphic Conditions, *Petrologiya*, 1994, vol. 2, no. 5, pp. 540–550.

Savko, K.A., Physicochemical Parameters of Metamorphism of Eulysites from the Central Part of the Voronezh Crystalline Massif, *Vestn. Voronezh. Univ., Geol.*, 1999, no. 8, pp. 73–81.

Savko, K.A. and Kal'mutskaya, N.Yu., Physicochemical Conditions of Metamorphism of Magnetite–Grunerite–Riebeckite Rocks at the Prioskol'skoe Iron Deposit, Kursk Magnetic Anomaly, *Vestn. Voronezh. Univ., Geol.*, 2002, no. 1, pp. 95–103.

Shchegolev, I.N., *Zhelezorudnye mestorozhdeniya dokembriya i metody ikh izucheniya* (Precambrian Iron Deposits and Methods of Their Study), Moscow: Nedra, 1985.

Spear, F.S. and Cheney, J.T., A Petrogenetic Grid for Pelitic Schists in the System SiO_2–Al_2O_3–FeO–MgO–K_2O–H_2O, *Contrib. Mineral. Petrol.*, 1989, vol. 101, no. 29, pp. 149–164.

Sudovikova, E.N., Green Mica from the Iron Ore Sequence of the Kursk Magnetic Anomaly, *Zap. Vses. Mineral. O–va*, 1956, part. 85, no. 4, pp. 543–549.

Trendall, A.F. and Blockley, J.G., The Iron Formation of the Precambrian Hamersley Group, Western Australia, with Special Reference to the Associated Crocidolite, *Western Australia Geol. Surv. Bull.*, 1970, p. 119.

Veres, G.I., Merenkova, T.B., and Ostrovskii, I.A., Artificial Pure Ferrous Hydroxyl Mica, *Dokl. Akad. Nauk SSSR*, 1955, vol. 101, no. 1, pp. 147–150.

Wones, D.R., Phase Equilibria of "Ferriannite," $K Fe_3^{+2} Fe^{+3} Si_3 O_{10}(OH)_2$, *Am. J. Sci.*, 1963, vol. 261, pp. 581–596.

Petrology, Vol. 11, No. 5, 2003, pp. 426–443. Translated from Petrologiya, Vol. 11, No. 5, 2003, pp. 471–490.

Riebeckite–Aegirine–Celadonite BIF at the Mikhailovskoe Iron Deposit of the Kursk Magnetic Anomaly: Phase Equilibria and Metamorphic Conditions

K. A. Savko and M. V. Poskryakova

Voronezh State University, Universitetskaya pl. 1, Voronezh, 394006 Russia
e-mail: gflab4@main.vsu.ru

Received August 10, 2002

Abstract—The Early Proterozoic banded iron formation (BIF) of the Mikhailovskoe iron deposit differs from other known Precambrian BIF by the low Al# and high $Fe^{3+}/(Fe^{3+} + Fe^{2+})$ ratios. The elevated oxygen fugacity during the metamorphic event and the Al-poor composition of the rocks were responsible for the origin of minerals high in Fe^{3+} and the absolute absence of Al-bearing phases. The BIF contains widespread celadonite, tetraferribiotite, Al-free chlorite, riebeckite, and aegirine instead of grunerite, stilpnomelane, minnesotaite, and greenalite, which are minerals usual in BIF elsewhere. Data on the phase equilibria provide information on the origin order of mineral assemblages and the physicochemical conditions of metamorphism. Its early stages were marked by the stability of quartz, carbonates, iron oxides, and potassic micas of specific composition. As the temperature increased, tetraferribiotite, celadonite, and riebeckite crystallized. Depending on the oxygen fugacity (above or below the hematite–magnetite buffer) in discrete layers, the *Aeg + Hem* and *Rbk + Mag* assemblages were formed. The metamorphic temperature was estimated at 370–520°C at a pressure of 2–3 kbar, Na activity $[\log[a(Na^+)/a(H^+)] = 5.5–6.0$, and oxygen fugacity above the hematite–magnetite buffer in layers with the *Aeg + Hem* assemblage and below this buffer in layers with *Rbk + Mag*.

INTRODUCTION

Banded iron formations (BIF) are an important constituent of all known Precambrian shields and the main indicator of the drastic change in the oxygen regime in the Earth's hydrosphere and atmosphere at the boundary between the Early and Late Proterozoic. Because of this, BIF were not found in complexes younger than 1.9 Ga. These unique Precambrian formations were studies by several researchers over many years. The main research avenues were the reconstruction of the sedimentation environments of the Fe-bearing rocks, analysis of their facies and formations, sources of the material, etc. At the same time, the evolution of BIF at the Kursk magnetic anomaly (KMA) was studied relatively poorly, mostly because of the following reasons:

* there is still no scheme of the facies and subfacies of Fe- and Si-rich rocks (contrary to, for example, metapelites);

* metamorphic zoning in rocks with such rare mineral assemblages was mapped very rarely (if at all);

* efforts to interpret the physicochemical metamorphic conditions of BIF were made based on very scarce experimental materials, particularly in the low- and medium-temperature regions, and these rocks contain no mineral assemblages that are conventionally utilized as geothermobarometers.

According to the chemical and mineralogic composition, BIF rocks are conventionally classed with one of the following four types of Fe–Si formations (James, 1954; Klein, 1973): (1) quartz–magnetite (hematite) type (which is also sometimes referred to as itabirite), containing the *Qtz–Mag*, *Qtz–Hem*, and *Qtz–Hem–Mag* assemblages; (2) quartz–carbonate, in which carbonates of the fero-dolomite–ankerite and siderite–pictomesite series are abundant; (3) quartz–silicate, which is dominated by quartz, Fe-rich phyllosilicates, such as greenalite, minnesotaite, chlorites (chamosite, clinochlore, ripidolite), micas (biotite, stilpnomelane, ferriannite), and, at higher metamorphic grades, grunerite, orthopyroxene, and fayalite; (4) Mn-rich BIF. Another type of widespread Early Proterozoic BIF at KMA are high-Fe riebeckite and aegirine-bearing rocks.

Thus, every type of high-Fe rocks is characterized by different mineral assemblages and, hence, their different evolutionary successions in the course of prograde metamorphism. Moreover, the stability of the mineral assemblages is strongly dependent on the oxygen fugacity, because of which a significant part in BIF metamorphism is played by redox reactions, which are particularly typical of low- and medium-temperature conditions. High-temperature metamorphism (to the high-temperature amphibolite and, particularly, granulite facies) of all of the aforementioned BIF types (except those high in Mn) results in magnetite–quartz–fayalite–orthopyroxene rocks, sometimes referred to as eulysites.

BIF rocks at the Mikhailovskoe iron deposit of KMA differ from other Precambrian BIF by low Al_2O_3 concentrations, even as compared with the generally low Al_2O_3 concentrations in all BIF rocks. This feature causes the complete absence of Al-bearing minerals. The phyllosilicates are K-bearing and virtually Al-free micas: celadonite and tetraferribiotite in place of stilpnomelane, minnesotaite, and greenalite, typical of BIF of low metamorphic grades. The wide occurrence of celadonite in association with tetraferribiotite, quartz, magnetite, and hematite at low metamorphic grades makes the Mikhailovskoe BIF different from other well-known Precambrian BIF at shields. The rocks also contain siderite, ankerite, Al-free chlorite, riebeckite, and aegirine.

This paper is centered on the succession of phase transitions in and the physicochemical metamorphic conditions of the tetraferribiotite–celadonite–riebeckite BIF at the Mikhailovskoe iron deposit, one of the largest in the world.

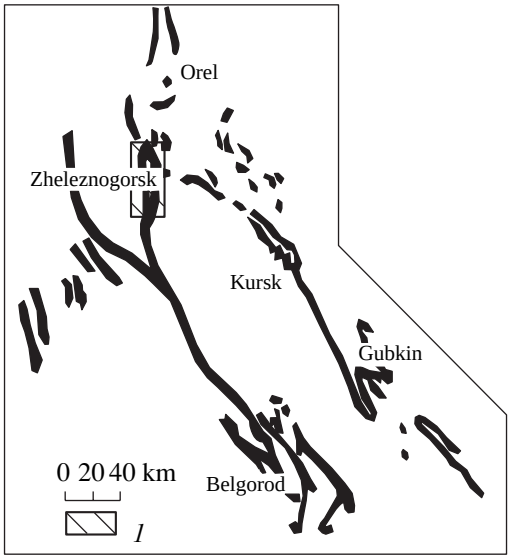

Fig. 1. Schematic map showing the distribution of the Early Proterozoic KMA BIF (after Shchegolev, 1985).
(*1*) Study area.

GEOLOGY

BIF were found in the KMA Precambrian at three stratigraphic levels: Early Archean, Late Archean, and Early Proterozoic. Archean BIF rocks occur locally, within small positive ellipsoidal, crescent-shaped, or stripe anomalies (Ushakovskoe, Kuvshinovskoe, Budanovskoe, Besedinskoe, and others) and consist of eulysites metamorphosed to the granulite facies. Their metamorphic parameters were assayed (Savko, 1999) at $T = 850°C$, $P = 5$ kbar, and $\log f_{O_2}$ from –14 to –15.

The Late Archean BIF rocks occur in greenstone belts in close association with amphibolites (Shchegolev, 1985). They compose elongated bodies up to 10 km long and relatively thin (no more than 100 m) and consist of quartz–magnetite–garnet–grunerite rocks. Their metamorphic parameters were determined at the Zapadnyi Kodentsovskii prospect as $T = 650 \pm 30°C$, $P = 5$ kbar, and $\log f_{O_2}$ from –17 to –20 (Savko, 1994).

The most widely spread BIF at KMA are of Early Proterozoic age (Kurskaya Group). The rocks compose two stripes (Shchigrovsko–Oskol'skaya and Mikhailovsko–Belomorskaya) trending roughly westward for more than 550 km (Fig. 1). All currently mined iron ores of KMA affiliate with the Early Proterozoic BIF.

We examined BIF rocks of the Mikhailovskoe ore field, whose central portion includes one of the worlds greatest Mikhailovskoe deposit (Fig. 2).

The deposit is hosted by Lower Proterozoic metamorphosed terrigenous–sedimentary rocks of the Kurskaya Group (Fig. 2). The group is subdivided into the sandy–shaly Stolenskaya and the BIF Korobkovskaya Formation. The Stoilenskaya Formation consists of a lower and upper subformations. In our study area, the rocks of the former are quartz conglomerates and quartz metasandstones with beds of almandine–chloritoid aluminous schists. The upper subformation consists of carbonaceous shales and barren quartzites. The Korobkovskaya Formation is subdivided into four subformations: lower iron-bearing, intermediate shaly, upper iron-bearing, and upper shaly. The lower iron-bearing subformation can be subdivided into four members: (1) magnetite quartzite, (2) magnetite–hematite quartzite, (3) hematite quartzite, and (4) intercalating magnetite and hematite quartzites.

BIF PETROGRAPHY AND CHEMISTRY

The rocks of the Korobkovskaya Formation at the Mikhailovskii mining district are dark gray and greenish gray fine-grained BIF, whose banding is accentuated by alternating mineralized (magnetite and hematite) and barren (quartz and silicate) layers (Fig. 3). The layers can have the following compositions: (a) quartz with magnetite, carbonate, and, sometimes, hematite (Borehole 3195); (b) hematite with quartz and, sometimes, magnetite, celadonite, and carbonates (sample MK-18); (c) silicate (riebeckite and celadonite) in association with hematite or magnetite (Boreholes 3830, 3829, 3291); and (d) magnetite with hematite, quartz, carbonates, and silicates (aegirine, riebeckite, and celadonite; Boreholes 3829, 3830, 3291). At the Mikhailovskoe Mine, BIF (which are sometimes plicated and crenulated) contain interbeds of variable composition: aegirine (up to 4 cm thick); aegirine–celadonite (up to 1.5–2 cm), riebeckite (0.5–1 cm), quartz–carbonate–celadonite (0.5–1 cm), magnetite (0.5–1 cm), and quartz–magnetite (1–2 cm) (Fig. 3).

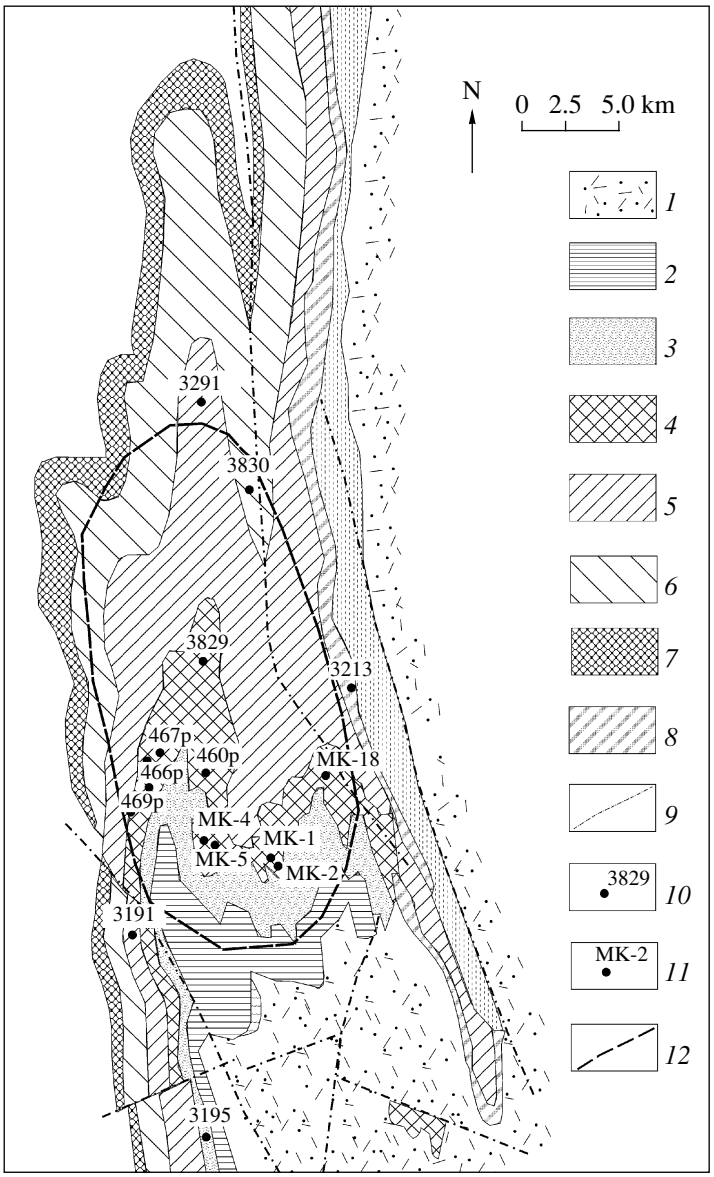

Fig. 2. Schematic geological map of the Mikhailovskoe iron deposit.

(*1*) Kurbakinskaya Formation: volcanomictic sandstone, shale, conglomerate, and quartz porphyry. Korobkovskaya Formation: (*2*) upper shale subformation (black carbonaceous quartz–chlorite–sericite shale), (*3*) upper iron ore subformation (magnetite, lean, red-banded hematite quartzite), (*4*) lower shale subformation (black carbonaceous quartz–chlorite–sericite shale and fine-grained sandstone), (*5*) lower iron ore subformation (magnetite and magnetite–hematite quartzite, red-banded hematite quartzite), (*6*) lower iron ore subformation, third unit (hematite–magnetite quartzite), (*7*) lower iron ore subformation, second unit (magnetite–hematite quartzite), (*8*) lower iron ore subformation, first unit (carbonate–magnetite, hematite–magnetite, and lean quartzite); (*9*) faults; (*10*) boreholes and their numbers; (*11*) sampling sites in the Mikhailovskii opencut mine; (*12*) contour of the Mikhailovskii opencut mine.

The mineralogy of BIF at the Mikhailovskoe iron deposit is controlled by the major-element chemistry and physicochemical metamorphic parameters. The chemistry of individual samples depends on the proportions of minerals composing the rocks. Chemical analyses of the Mikhailovskoe BIF are listed in Table 1 and generally correspond to the average composition of BIF from known iron-ore basins (Gole and Klein, 1981), except only for the FeO and Fe_2O_3 concentrations. The Mikhailovskoe BIF are noted for the strong predominance of Fe_2O_3 over FeO, with the $Fe^{3+}/(Fe^{3+} + Fe^{2+})$ ratios ranging from 0.70 to 0.87 (averaging 0.76) at elevated total Fe concentrations (ΣFe = 37.1–40.47 wt % at an average of 38.7 wt %). In a review of the chemical compositions of rocks from five Proterozoic BIF (Gole and Klein, 1981), the average value of the $Fe^{3+}/(Fe^{3+} + Fe^{2+})$ ratio does not exceed 0.5, ranging from 0.31 in the Marra Mamba Iron Formation in western Australia to 0.45–0.46 in formations of the Labrador Trough, Canada, and Biwabik in Minnesota, at total iron concentra-

tions of 30–32 wt %. Hence, the Mikhailovskoe BIF are characterized by a high average oxidation state of iron and its elevated overall concentrations compared with BIF elsewhere. The average K_2O and Na_2O concentrations in the rocks are closely similar to those in BIF in western Australia (Hamersley Basin, Marra Mamba) and are slightly higher than in BIF in North America.

We obtained microprobe analyses of minerals in the Early Proterozoic BIF from the Mikhailovskoe iron deposit. The mineral assemblages of these rocks are listed in Table 2, and the sampling sites are shown in Fig. 2.

METHODS

The more than 120 BIF samples are fragments of borehole core and specimens taken in the walls of the Mikhailovskoe opencut mine, which were described in much detail in field. The petrographic thin sections prepared from these samples were examined optically and analyzed at a Camebax SX-50 microprobe at the Moscow State University. The operating conditions were 15 kV accelerating voltage, 1–2 nA beam current, and 1–2 μm beam diameter. The analytical accuracy was systematically controlled by the analyses of natural and synthetic standards. The BSE images of thin sections were taken on a CamScan electron microscope with a Link EDS analytical set at the Moscow State University. The crystal chemical formulas of minerals were normalized to 6 oxygen atoms for aegirine, 23 for riebeckite, 11 for micas, 14 for chlorites, 8 for potassium feldspar, and 4 for magnetite.

Fig. 3. BIF at the sampling site MK-18 in the Mikhailovskii iron ore opencut mine.

Dark layers are magnetite–celadonite–riebeckite and magnetite–hematite–celadonite–aegirine BIF varieties.

MINERALOGY

Magnetite is the main ore- and rock-forming mineral and occurs as individual grains of various size and octahedral habit, which are commonly concentrated within thin layers and lamina up to a few millimeters thick. This mineral is present in virtually all rock types, and its amount attains 50 modal %. The composition corresponds to pure magnetite, with the MgO, MnO, SiO_2, and Al_2O_3 admixtures amounting to no more than a few tenths of a percent (Table 3).

Hematite is always quantitatively subordinate to magnetite and occurs as platelets and flakes ranging from fractions of a millimeter to a few millimeters. Small hematite flakes are usually grouped within thin lamina up to a few millimeters thick, which are parallel to the rock bedding.

Table 1. Chemical composition of BIF from the Mikhailovskoe deposit

Component	712	714	715	716/1	716/2	717/1	717/2	718/1	718/2	719	720	801
SiO_2	38.76	38.30	40.74	39.76	39.10	39.06	42.34	40.38	39.62	38.72	38.16	38.06
TiO_2	0.49	0.23	0.25	0.25	0.30	0.35	0.30	0.25	0.27	0.47	0.46	0.47
Al_2O_3	0.01	0.56	0.57	0.53	0.49	0.53	0.65	0.49	0.47	0.01	0.13	0.01
Fe_2O_3	50.26	43.18	39.44	39.40	45.40	38.91	35.90	38.26	42.77	43.90	44.91	41.88
FeO	6.85	11.42	12.50	13.41	10.34	13.69	13.65	14.21	11.05	11.58	11.49	14.06
MnO	0.01	0.03	0.05	0.02	0.02	0.03	0.03	0.03	0.02	0.02	0.03	0.02
MgO	0.35	1.08	1.04	1.18	0.61	1.24	1.24	1.25	1.08	1.07	0.11	1.42
CaO	1.59	0.78	0.91	0.98	0.77	1.26	1.24	1.21	0.98	1.13	1.08	1.19
Na_2O	0.04	0.30	0.38	0.85	0.20	0.55	0.40	0.55	0.37	0.48	0.35	0.61
K_2O	0.30	0.93	1.10	1.08	0.80	1.20	1.22	0.85	0.83	1.05	0.80	0.97
Total	98.66	96.81	96.98	97.46	98.03	96.82	96.97	97.48	97.46	98.43	98.52	98.69
ΣFe	40.47	39.08	37.31	37.98	39.79	37.85	35.72	37.81	38.50	39.71	40.43	40.22
$Fe^{3+}/(Fe^{3+} + Fe^{2+})$	0.87	0.77	0.74	0.73	0.80	0.72	0.70	0.71	0.78	0.77	0.78	0.73

Note: Analyses were conducted at the chemical laboratory of NPO Tsentrgeologiya.

Table 2. Mineralogic composition of BIF from the Mikhailovskoe deposit

Mineral	*Qtz*	*Mag*	*Hem*	*Sld*	*Bt*	*Chl*	*Ank*-Fe-*Dol*	*Sd*	*Aeg*	*Rbk*
MK-1	+	+	+	+	+	–	+	+	+	*
MK-2	+	+	+	+	–	+	–	–	–	+
MK-4	+	+	+	+	–	+	–	–	+	*
MK-5	+	+	+	+	–	–	+	+	+	–
MK-15	+	+	+	+	–	–	+	+	+	–
MK-18	+	+	+	+	–	–	–	–	+	–
3195/15	+	+	–	+	–	–	+	+	+	+
3213/8	+	+	+	+	+	+	+	+	+	*
3291/479	+	+	+	+	+	–	–	–	–	–
3829/2	+	+	+	+	s.g.	+	+	+	+	s.g.
3829/4	+	+	+	*	+	–	–	inc.	+	inc.
3829/6	+	+	+	+	s.g.	+	+	+	–	–
3829/7	+	+	+	+	–	–	–	+	+	inc., *
3830/14	+	+	+	+	–	–	+	+	+	–
3830/16	+	+	+	+	–	–	+	+	+	–
3830/21	+	+	–	+	+	–	–	–	–	+
3830/23	+	+	+	+	+	s.g.	+	+	–	+
3830/28	+	+	+	+	–	–	–	–	–	+
3830/29	+	+	+	+	inc.	–	+	+	+	*
3830/30	+	+	+	+	+	–	+	+	+	–
3830/31	+	+	+	–	+	+	–	–	–	+
3830/32	+	+	+	+	+	–	+	+	–	+
3830/39	+	+	+	+	+	+	+	+	+	–
3830/40	+	+	+	+	inc.	inc.	–	–	+	*
3830/47	+	+	+	+	inc.	+	+	+	+	inc.
3830/49	+	+	+	+	–	+	+	+	+	–
3830/58	+	+	–	+	–	–	+	+	–	+
3830/59	+	+	+	–	–	–	+	+	+	–
460p/86	+	+	+	+	–	–	+	+	+	–
466p/32	+	+	+	+	–	+	–	–	–	+
466p/100	+	+	–	+	–	+	+	+	–	+
466p/130	+	+	+	+	–	+	+	+	–	+
466p/131	+	+	+	+	inc.	inc.	+	+	+	–
467p/195	+	+	+	–	–	+	+	+	–	+
467p/205	+	+	+	–	–	+	+	+	+	–
467p/214	+	+	–	+	–	–	–	–	–	+
467p/217	+	+	+	–	–	+	+	+	–	+
469p/254	+	+	+	+	–	–	–	–	–	–

Note: Abbreviations: s.g—single grain, inc.—inclusion in aegirine; *secondary.

In addition to quartz and magnetite, hematite is usually accompanied by aegirine and phyllosilicates. Most samples show evidence of magnetite martitization, i.e., its replacement by pseudomorphs of secondary hematite.

Micas. The Mikhailovskoe BIF contain Fe-rich micas, which are either the only or the predominant silicates of most BIF varieties. We identified tetraferribiotite and celadonite.

Table 3. Chemical composition of carbonates and magnetite in BIF from the Mikhailovskoe deposit

Component	3830/58				3830/14			MK-18	3195/15	3291/479	460p/86.0		466p/131.0	
	Mag-7	*Dol*-8*	*Sd*-10	*Ank*-51	*Mag*-49	*Sd*-24	*Dol*-29	*Mag*-26	*Dol*-71	*Mag*-9	*Sd*-8	*Dol*-15	*Dol*-13	*Sd*-21
SiO_2	0.07	0.24	0.14	0.28	1.32	0.17	0.43	1.08	0.41	0.11	0.26	0.24	0.31	0.09
TiO_2	–	0.04	–	–	–	–	0.14	–	–	–	–	–	–	–
Al_2O_3	0.09	0.26	0.2	0.11	–	–	–	0.18	–	–	0.13	–	0.02	–
FeO	99.74	19.46	64.99	37.05	97.29	66.64	22.61	98.15	21.22	99.57	73.34	23.98	24.65	76.60
MnO	0.02	0.6	1.39	0.5	–	0.24	0.03	–	0.72	0.09	2.03	0.90	1.08	1.24
MgO	–	26.78	32.9	14.28	0.34	32.04	25.74	0.09	25.92	0.02	23.11	24.04	23.61	21.40
CaO	0.02	52.55	0.36	47.38	0.06	0.68	50.52	–	51.68	–	0.46	50.14	50.20	0.28
Na_2O	–	–	–	–	–	0.23	0.24	0.05	0.05	–	0.61	0.37	0.08	0.35
K_2O	–	0.07	0.01	0.01	–	–	0.07	0.15	–	–	0.03	0.30	–	–
Total	99.94	100.00	100.00	100.00	99.01	100.00	99.99	99.70	100.00	99.98	99.97	99.97	99.95	99.96
Si	0.03	–	–	–	0.05	–	–	0.04	–	–	–	–	–	–
Al	0.04	–	–	–	–	–	–	0.01	–	–	–	–	–	–
Ti	–	–	–	–	–	–	–	–	–	–	–	–	–	–
Fe^{3+}	1.90	–	–	–	1.90	–	–	1.95	–	1.01	–	–	–	–
Fe^{2+}	1.03	0.14	0.51	0.29	1.03	0.53	0.17	0.97	0.16	0.97	0.62	0.18	0.19	0.66
Mn	–	–	0.01	–	–	–	–	–	0.01	–	0.02	0.01	0.01	0.01
Mg	–	0.35	0.46	0.20	0.02	0.46	0.34	0.01	0.34	–	0.35	0.32	0.32	0.32
Ca	–	0.49	–	0.49	–	0.01	0.48	–	0.49	–	0.01	0.48	0.48	–
Na	–	–	–	–	–	–	–	0.02	–	0.22	0.01	0.01	0.01	–
K	–	–	–	–	–	–	–	0.01	–	–	–	–	–	–
X_{Fe}		0.29	0.53	0.59		0.54	0.33		0.32		0.64	0.36	0.37	0.67

* All analyses are normalized to 100%. Here and in Tables 4–7, dashes mean concentration below the analytical determination limit, n.a.—not analyzed; $X_{Fe} = Fe^{2+}/(Fe^{2+} + Mg)$; oxides are given in wt %.

Tetraferribiotite is a fairly rare Al-free mica, which has the formula $K(Mg, Fe^{2+}, Fe^{3+})_3[Fe^{3+} Si_3O_{10}](OH)_2$ and was discovered in 1955 during an unsuccessful experimental effort to synthesize K–OH amphibole (Veres *et al.*, 1955). One member of the tetraferribiotite group, ferriannite, was obtained in the experiments of Wones (1963) within the temperature range of 400–850°C, pressures of 1035–2070 bar, and an oxygen fugacity between the hematite–magnetite and iron–wuestite buffers. Wones explored the hypothesis that mica of ferriannite composition should occur in magmatic Fe-rich rocks. Later ferriannite was described in riebeckite-bearing rocks in iron formations in western Australia (Miyano and Miyano, 1982; Miyano, 1982) and South Africa (Miyano and Beukes, 1997). Micas of the tetraferriannite–tetraferriphlogopite isomorphous series were described in the iron formation of the Kursk Magnetic Anomaly as early as the 1950–1960s (Sudovikova, 1956; Illarionov, 1965).

Tetraferribiotite occurs in the iron formation of the Mikhailovskoe mining district in the form of small brownish flakes 0.2–1.0 mm across (Fig. 4b) approximately in every fourth sample, in which it is accompanied by magnetite, hematite, riebeckite, aegirine, celadonite, and carbonate. The mineral occurs in subordinate amounts compared with celadonite and is preferably localized in magnetite–hematite layers as disseminated flakes, although can occasionally also compose nearly monomineralic thin layers with merely minor amounts of celadonite and iron oxides. Tetraferribiotite sometimes forms inclusions in aegirine (Figs. 5a, 5d, 6a), although these rocks may contain no this mineral in the groundmass. When in magnetite–hematite layers, tetraferribiotite is commonly replaced by celadonite (Fig. 4b).

Tetraferribiotite in the KMA iron formation is less aluminous (Table 4; Al_2O_3 = 0.68–0.76 wt %) and more magnesian (MgO = 10.13–14.09 wt %) than natural ferriannite (Miyano and Miyano, 1982; Miyano and Beukes, 1997), whose Al_2O_3 content is always higher than 1.3 wt %, usually about 4–5 wt %, and the MgO concentration varies from 3.5 to 12.5 wt % (Fig. 7). The Si/Al ratio of the tetraferribiotite is always one order of magnitude higher: 3.0. The least aluminous tetraferribiotite was detected as inclusions in aegirine. Hence, the compositions of the KMA tetraferribiotite are most

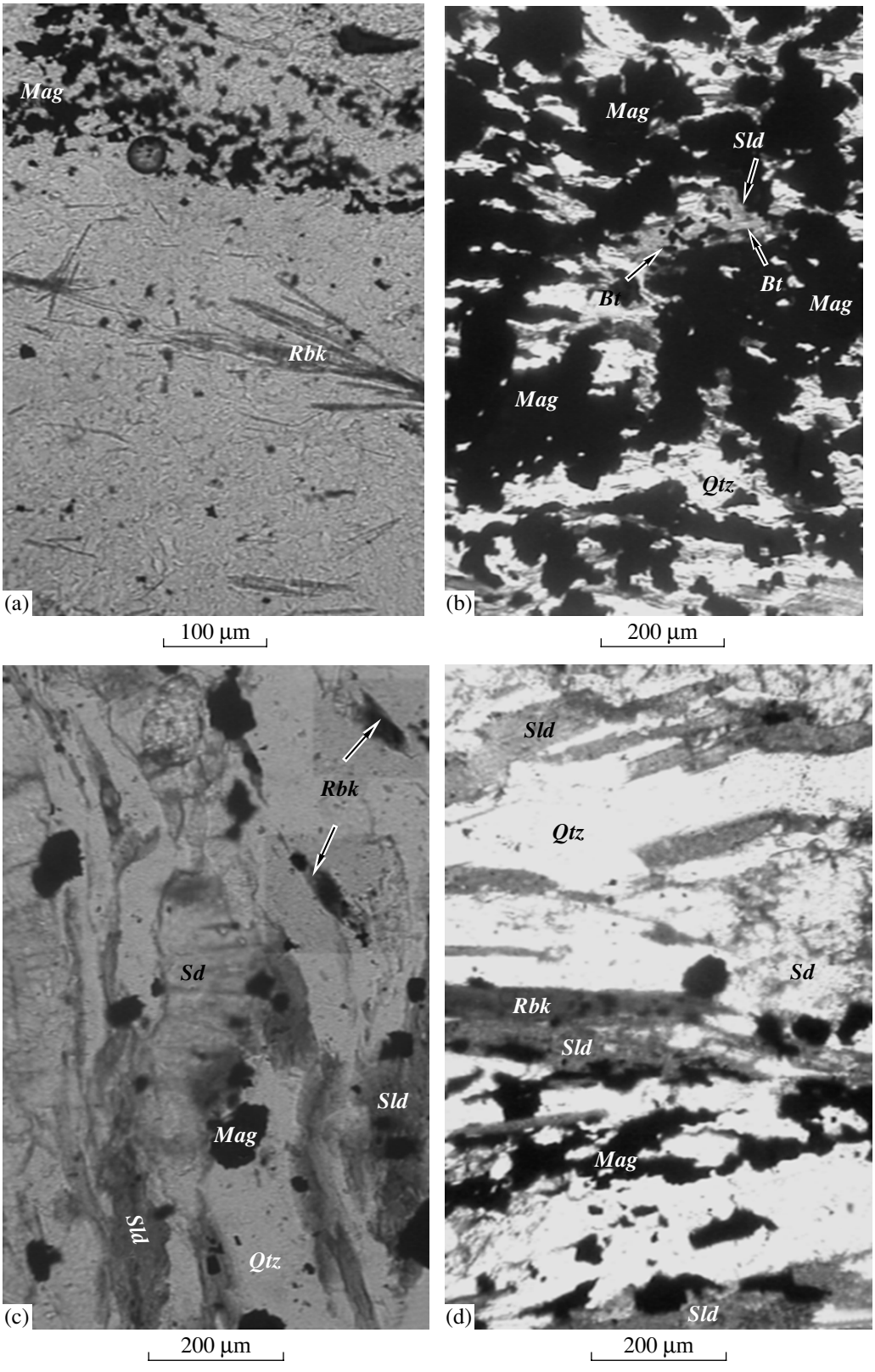

Fig. 4. Micrographs of reaction textures in BIF from the Mikhailovskoe iron deposit.
(a) Acicular riebeckite crystals develop in a quartz–magnetite matrix, sample 467r/214; (b) tetraferribiotite (light gray) is replaced by celadonite (dark gray) in the margins in a magnetite layer, sample 3830/21; (c) celadonite and riebeckite replace siderite, sample 3830/28; (d) celadonite is replaced by riebeckite, sample 3830/28. All micrographs were taken with one polarizer.

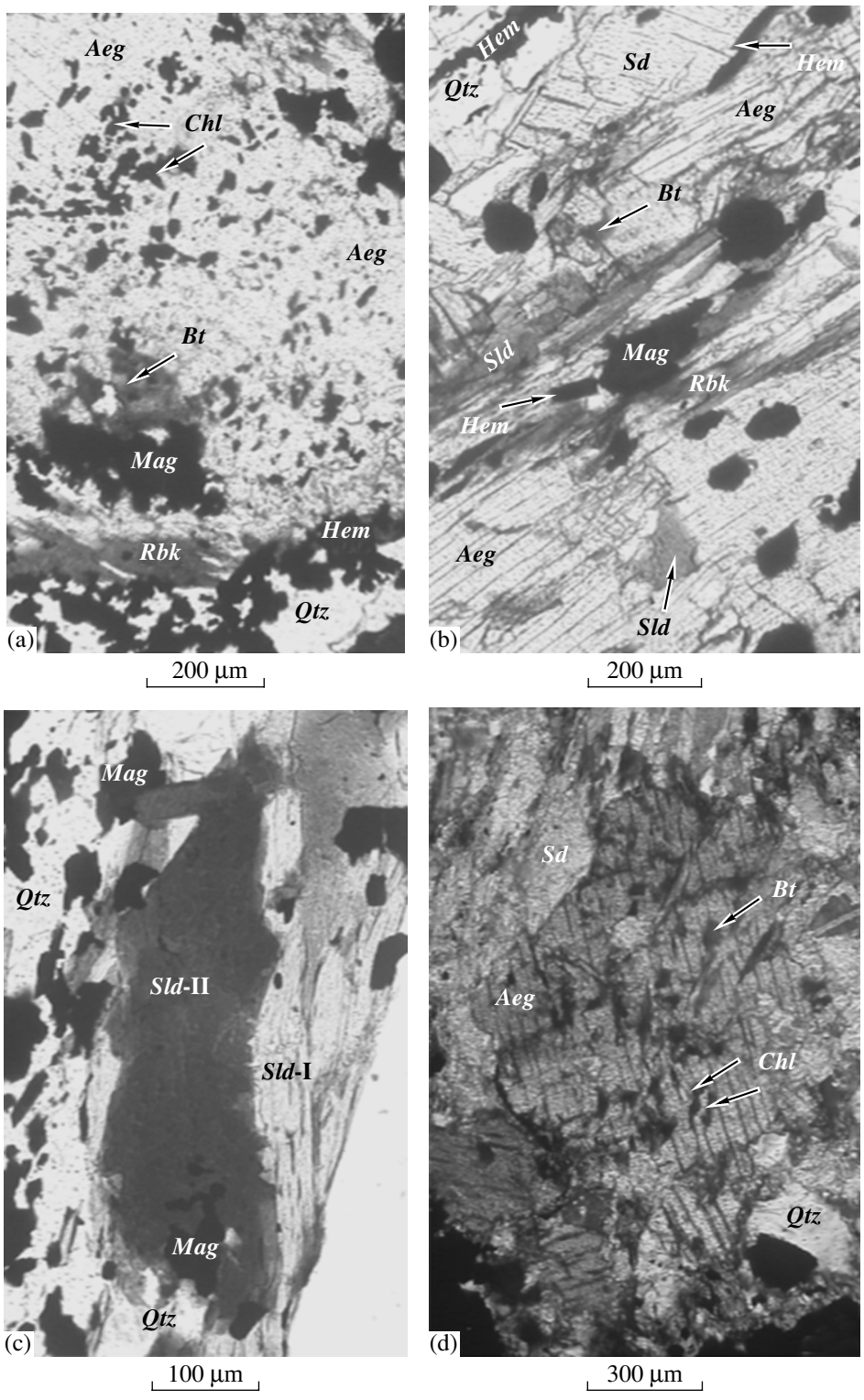

Fig. 5. Micrographs of reaction textures in BIF from the Mikhailovskoe iron deposit.

(a) Large aegirine grain with tetraferribiotite, chlorite, and magnetite inclusions; aegirine is replaced by retrograde riebeckite in the margins, sample 3830/29. (b) Siderite is replaced by aegirine, the latter contains celadonite inclusions and is replaced by retrograde riebeckite along cracks, sample 3830/40. (c) Two populations of celadonite, sample 3830/49. (d) Large aegirine crystals grow in carbonate domains, the aegirine contains tetraferribiotite and chlorite inclusions, sample 3829/7 (one polarizer). (e) Riebeckite develops in celadonite layers, sample 466r/100.

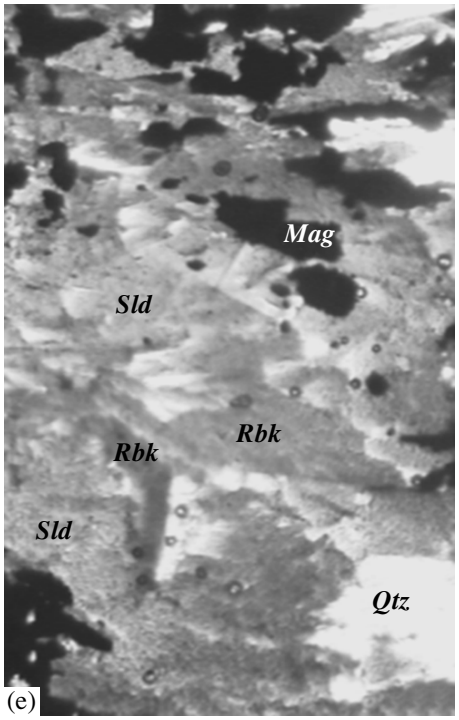

Fig. 5. (Contd.)

close to that of the end member of the annite–ferriannite series and shift toward tetraferriphlogopite in the tetraferriannite–tetraferriphlogopite series (Fig. 7). The KMA tetraferribiotite is also noted for an elevated MnO concentration (up to 0.66 wt %) as compared with those in ferriannite from other iron formations (which contains no more than 0.1 wt %).

The iron formations at the Mikhailovskii prospect of KMA usually contain another green mica, whose composition corresponds to *celadonite*, having the formula $KFe^{3+}(Mg, Fe^{2+})\square[Si_4O_{10}](OH)_2$ (Rieder *et al.*, 1999).

Dioctahedral micas were first studied in the KMA BIF in the 1950–1960s (Sudovikova, 1956; Illarionov, 1965; Foster, 1959). E.N. Sudovikova described a green mica in the KMA BIF in 1956. The mica was in assemblage with aegirine and alkaline amphibole. Mega- and microscopic research led her to ascribe this mica to the phlogopite–lepidomelane series. Later M. Foster (1959) arrived at the conclusion that the green mica from the KMA BIF is not trioctahedral, because its crystal chemical formula appeared to be close to that of dioctahedral potassic mica celadonite.

Celadonite is present in most of our samples, occurring as flakes of emerald green color, ranging from a few tenths of a millimeter to 1.5–2 mm, whose amount sometimes attains 30–40 modal % (Figs. 4d, 5e, 6b–6d).

Celadonite occurs in interlaced aggregates with riebeckite (Fig. 5e), and their crystals (platelets and tables; Fig. 6d, 6e) in magnetite layers are larger than in quartz layers. Aggregates of celadonite and riebeckite can develop as rims around large carbonate grains and separate them from the granoblastic quartz aggregate. Riebeckite sometimes pseudomorphs celadonite (Fig. 4d), or tiny riebeckite needles ("nuclei") occur between magnetite and celadonite grains. Celadonite flakes often develop after carbonate (Fig. 4c). Carbonate domains and the quartz matrix are separated by magnetite–celadonite intergrowths.

The celadonite is very low in Al, has a relatively high X_{Fe} (equal to 0.27–0.41; Table 5), and approaches ferroceladonite of the celadonite–ferroceladonite series (Fig. 8).

The celadonite can be subdivided into two textural groups (Fig. 5c). Celadonite in association with aegirine is usually anhedral, cloud-shaped, while this mineral in the absence of aegirine is mostly platy. Anhedral celadonite develops in cleavage fractures of the platy celadonite. Optically, the platy and anhedral celadonites are also different: when platy, this minerals is pleochroic from dark green to pale yellow or greenish yellow, while the anhedral celadonite, composing irregularly shaped aggregates without visible cleavage, is pleochroic from emerald green to green. The two types of celadonite have practically identical compositions.

Chlorite develops as small (no more than 0.5 mm) reddish brown crystals, which were found exclusively in hematite–magnetite layers free of carbonates or as inclusions, together with magnetite, in aegirine. In the latter situation, chlorite inclusions are restricted to the marginal portions of aegirine crystals, whereas chlorite is absent at aegirine contacts with hematite and from the groundmass (Figs. 5a, 5d, 6a).

Chlorite in the Mikhailovskoe BIF is usually practically free of Al_2O_3 (<0.5 wt %) and is high in Fe^{3+} (Table 4), with X_{Fe} = 0.54–0.67. Hence, the chlorite composition corresponds to ferrichamosite, a hypothetical end member of the chamosite–ferrichamosite series and a member of the ferriclinochlore–ferrichamosite series (Burt, 1989).

Riebeckite occurs in two morphological types. Type I composes elongated prismatic crystals up to 2–5 mm long, of bluish green color with noticeable pleochroism from greenish gray to bluish green and bluish yellow, composing layers of bright blue color up to 1 cm thick (Fig. 6c). The other morphological type of riebeckite comprises acicular aggregates and sheaves of bluish crystals or chains of dark blue crystals 0.5–1 mm long (Fig. 4a) pleochroic from colorless to dark blue.

Riebeckite develops as pseudomorphs after celadonite and tetraferribiotite (Figs. 4d, 5e) and is usually restricted to magnetite layers or carbonate domains. It is also common as inclusions in aegirine and, in these rocks, is absent from their groundmass. Finely acicular riebeckite can replace aegirine along cleavage planes (Figs. 5a, 5b).

Riebeckite in the Mikhailovskoe BIF is fairly magnesian (X_{Fe} = 0.36–0.66, Table 6) and, except for three

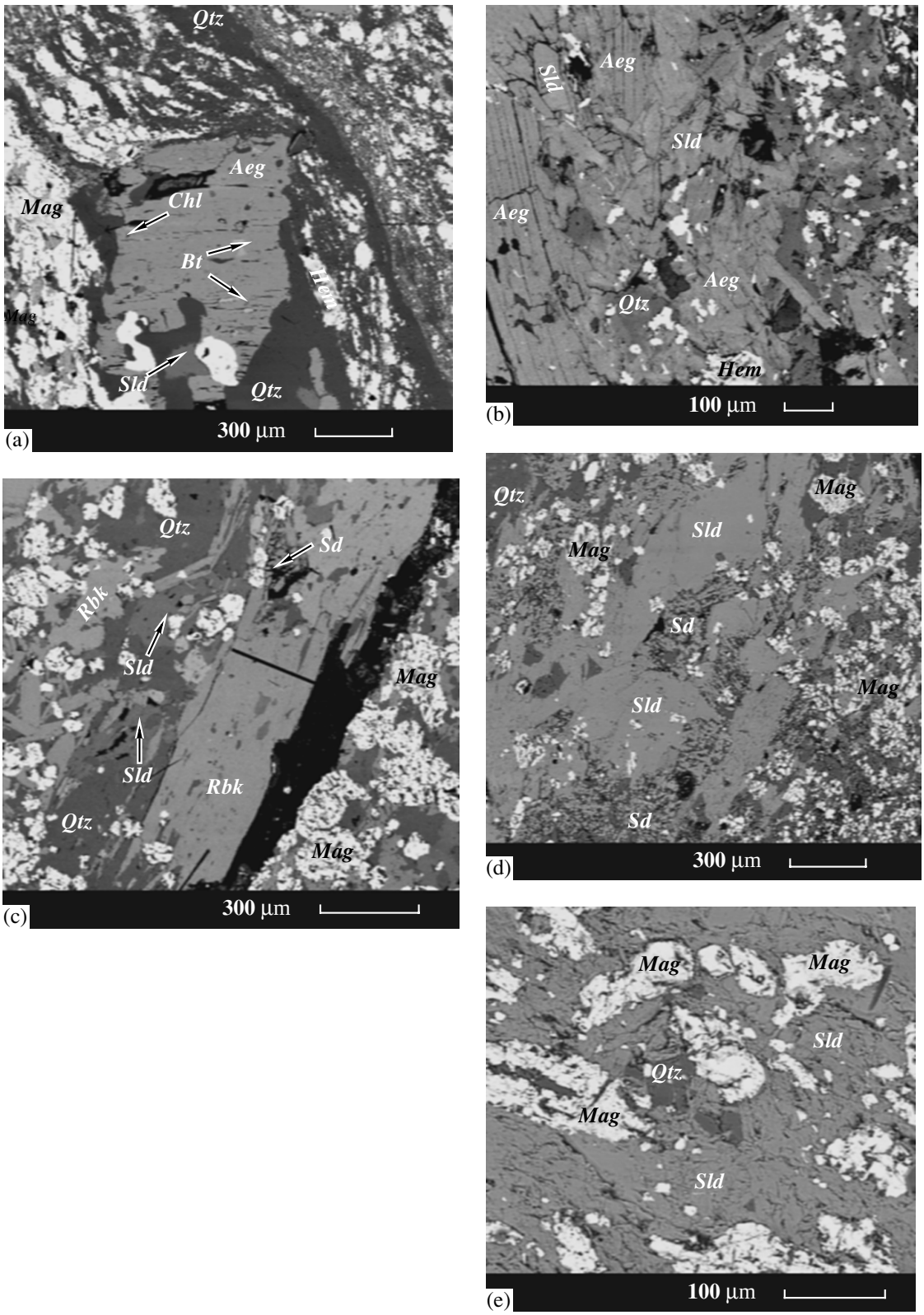

Fig. 6. BSE images of thin sections of BIF from the Mikhailovskoe iron deposit.

(a) Large aegirine grain with tetraferribiotite and chlorite inclusions, sample 3213/8. (b) Intergrowths of celadonite with aegirine, sample 3830/14. (c) Large riebeckite crystal with siderite inclusions, sample 3830/58. (d) Celadonite grows in a quartz–magnetite matrix, sample 460r/86. (e) Celadonite layer in BIF; celadonite develops at the sacrifice of quartz and magnetite.

Table 4. Chemical composition of tetraferribiotite, chlorite, and microcline in BIF from the Mikhailovskoe deposit

Component	3213/8			3291/479.0						3213/8			
	incl. in *Aeg*			matrix						incl. in *Aeg*	matrix		
	Chl-32	*Chl*-34	*Chl*-42	*Bt*-1	*Bt*-2	*Bt*-3	*Bt*-8	*Kfs*-5	*Kfs*-7	*Bt*-20	*Bt*-21	*Bt*-23	*Bt*-25
SiO_2	25.18	24.73	24.39	38.48	37.52	38.26	37.61	63.99	64.09	37.46	37.65	36.92	38.66
TiO_2	0.02	0.02	–	0.37	0.43	0.35	0.40	–	0.03	0.01	–	–	0.04
Al_2O_3	0.24	0.20	0.42	0.71	0.68	0.68	0.76	16.02	16.46	0.53	0.88	1.12	2.60
FeO	51.47	49.45	47.31	31.61	31.49	30.13	32.18	3.01	2.74	37.13	38.43	43.70	29.60
MnO	0.05	–	0.07	0.66	0.51	0.50	0.66	–	0.05	0.23	0.15	0.01	0.12
MgO	9.02	9.61	12.53	14.09	12.69	13.69	12.53	–	–	10.86	10.13	4.45	12.43
CaO	0.18	0.12	0.11	0.02	–	0.11	–	0.03	0.01	0.50	0.20	0.02	0.25
Na_2O	0.03	0.01	0.03	0.02	0.01	0.05	0.03	0.09	–	0.06	0.15	–	0.04
K_2O	0.11	0.12	0.12	9.35	8.98	8.68	9.26	16.84	16.58	7.59	8.11	7.35	8.90
F	n.a.	n.a.	n.a.	0.24	0.03	0.10	0.23	n.a.	n.a.	n.a.	n.a.	n.a.	n.a.
Cl	n.a.	n.a.	n.a.	0.03	0.03	0.05	0.01	n.a.	n.a.	n.a.	n.a.	n.a.	n.a.
Total	86.30	84.26	84.98	95.48	92.37	92.60	93.67	99.99	99.95	94.37	95.70	93.57	92.64
	14O			11O				8O		11O			
Si	3.06	3.06	2.93	3.09	3.14	3.17	3.11	2.99	2.99	3.13	3.11	3.25	3.20
Ti	–	–	–	0.02	0.03	0.02	0.02	–	–	–	–	–	–
Al(IV)	0.04	0.03	0.06	0.07	0.07	0.07	0.07	0.88	0.91	0.05	0.09	0.12	0.25
Fe^{3+}	1.87	1.88	2.12	0.84	0.79	0.76	0.82	0.12	0.11	0.82	0.80	0.63	0.55
Fe^{2+}	3.35	3.23	2.62	1.45	1.63	1.61	1.58	–	–	1.82	1.85	2.59	1.49
Mn	0.01	–	0.01	0.04	0.04	0.04	0.05	–	–	0.02	0.01	–	0.01
Mg	1.63	1.77	2.24	1.69	1.58	1.69	1.54	–	–	1.35	1.25	0.58	1.53
Ca	0.03	0.02	0.02	–	–	0.01	–	–	–	0.04	0.02	–	0.02
Na	0.01	–	0.01	–	–	0.01	–	0.01	–	0.01	0.02	–	0.01
K	0.02	0.02	0.02	0.96	0.96	0.92	0.98	1.00	0.99	0.81	0.85	0.83	0.94
F	–	–	–	0.06	0.01	0.03	0.06	–	–	–	–	–	–
Cl	–	–	–	–	–	0.01	–	–	–	–	–	–	–
X_{Fe}	0.67	0.65	0.54	0.46	0.51	0.49	0.51			0.57	0.60	0.81	0.49

analyses, corresponds to magnesioriebeckite in the classification of Leake *et al.* (1997) (Fig. 9). The MgO concentration ranges within 4.46–9.03 wt %, which is higher than that of riebeckite from other iron formations. For example, according to Robinson *et al.* (1982), this mineral from iron formations contains 1.37–7.71 wt %, although magnesioriebeckite was found in the iron formation of southwestern Labrador (MgO = 17.0 wt %; Klein, 1966).

Aegirine in the iron formation of the Mikhailovskii district forms prismatic crystals 3–4 mm long, which compose layers of grass green color 1–2 cm thick (up to 4 cm in swells) in BIF (Figs. 3, 5a). Aegirine crystals sometimes develop as masses of sheaf-shaped aggregates (Fig. 6b).

Aegirine crystallizes in magnetite and carbonate layers (Fig. 6a). This mineral is rarely accompanied by riebeckite, and, in this situation, riebeckite usually replaces aegirine in the margins and along cracks (Figs. 5a, 5b). The aegirine contains inclusions of chlorite, celadonite, riebeckite, and tetraferribiotite (Figs. 5a, 5b, 5d, 6a). Most samples with aegirine from metalliferous layers contain hematite.

The aegirine is low in Al_2O_3 (0.02–0.12 wt %), TiO_2 (no more than 0.10 wt %), CaO (0.02–0.31 wt %), MgO (no more than 0.17 wt %), and MnO (no more than 0.21 wt %) (Table 7) and corresponds to the end member of the aegirine–augite series.

Carbonates of the iron formation at the Mikhailovskoe deposit composes layers up to 1–2 cm thick and lenses and domains of nearly oval shape. The carbonates develop as equant or elongated grains 0.2–0.7 mm and belong to the ankerite–ferrodolomite series or are dolomite (Table 3). Carbonates of the ferrodolo-

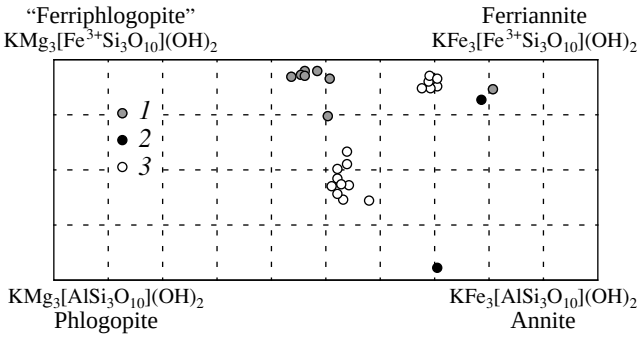

Fig. 7. Compositions of tetraferribiotite shown in a classification plot.
Rocks containing tetraferribiotite: (*1*) BIF from the Mikhailovskoe deposit; (*2*) Penge iron formation, South Africa; (*3*) Dales George, West Australia.

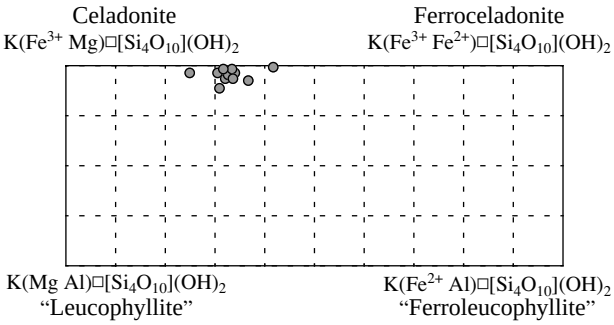

Fig. 8. Compositions of celadonite shown in a classification plot.

mite–ankerite series have Fe/(Fe + Mg) = 0.29–0.59, with most of the values ranging from 0.32 to 0.37. The siderite is more ferrous: Fe/(Fe + Mg) = 0.53–0.67. Siderite is common in oxidized varieties of BIF, and ankerite and dolomite are usually accompanied by magnetite, celadonite, riebeckite, and aegirine (Figs. 4c, 4d, 5b). Siderite inclusions are sometimes contained in large riebeckite crystals (Fig. 6c). The siderite and ankerite contain minor MgO admixtures, up to 1.24 wt % (Table 3).

Potassic feldspar (microcline) is a very rare mineral and was found only in four samples in association

Table 5. Chemical composition of celadonite in BIF from the Mikhailovskoe deposit

Component	466p/131.0		469p/254.0		460p/86			MK-1	
	2	3	1	3	1	2	3	1	2
SiO_2	50.49	50.85	51.58	51.15	50.79	50.97	50.72	51.09	51.72
TiO_2	0.01	0.01	–	–	0.01	–	0.01	0.01	–
Al_2O_3	0.49	0.35	0.49	0.12	0.54	0.84	1.35	0.12	0.49
FeO	26.15	26.07	25.80	26.01	25.67	26.73	26.32	26.67	25.68
MnO	–	–	–	0.01	0.02	0.01	–	0.02	0.01
MgO	4.80	4.90	4.68	4.59	5.02	4.54	4.34	4.62	4.58
CaO	0.05	0.01	–	–	0.01	0.02	0.01	0.01	0.02
Na_2O	0.05	0.04	–	0.06	–	0.02	0.02	–	0.02
K_2O	10.66	10.35	10.64	10.24	10.54	10.90	10.82	10.80	10.84
Total	92.70	92.58	93.19	92.18	92.60	94.03	93.59	93.34	93.36
				11O					
Si	3.77	3.80	3.83	3.85	3.79	3.76	3.75	3.80	3.83
Ti	–	–	–	–	–	–	–	–	–
Al(VI)	0.04	0.03	0.04	0.01	0.05	0.07	0.12	0.01	0.04
Fe^{3+}	1.44	1.36	1.30	1.28	1.37	1.44	1.40	1.42	1.32
Fe^{2+}	0.19	0.27	0.30	0.35	0.22	0.20	0.23	0.24	0.27
Mn	–	–	–	–	–	–	–	–	–
Mg	0.53	0.55	0.52	0.51	0.56	0.50	0.48	0.51	0.51
Ca	–	–	–	–	–	–	–	–	–
Na	0.01	0.01	–	0.01	–	–	–	–	–
K	1.01	0.99	1.01	0.98	1.00	1.02	1.02	1.02	1.02
X_{Fe}	0.27	0.33	0.37	0.41	0.29	0.29	0.32	0.32	0.35

Table 6. Chemical composition of riebeckite in BIF from the Mikhailovskoe deposit

Component	MK-2				3830/58							3195/15			
	incl. in *Aeg*		matrix		profile across a large riebeckite crystal						matrix	matrix			
	41	43	45	48	margin	→	core	→	→	margin	9	61	63	67	69
SiO_2	52.70	52.24	52.49	52.71	54.31	53.17	54.26	54.15	53.79	53.85	53.90	53.56	54.26	53.66	54.20
TiO_2	–	–	0.01	0.01	0.01	–	0.05	–	0.06	–	–	0.36		0.03	0.05
Al_2O_3	0.01	0.04	0.02	–	0.53	0.09	0.16	0.68	0.61	0.53	0.51	–	0.71	0.06	0.17
FeO	31.02	30.85	33.65	31.28	28.02	27.06	26.19	27.53	28.08	28.23	27.58	27.93	26.61	28.82	26.94
MnO	0.01	0.01	–	0.05	–	–	–	–	–	–	0.11	0.09	–	–	0.04
MgO	6.32	6.61	4.46	6.06	7.91	8.72	9.03	8.17	7.66	7.85	7.99	8.01	8.67	7.29	8.76
CaO	0.12	0.03	0.02	0.09	0.04	0.09	0.12	0.17	0.14	0.04	0.15	0.01	0.07	0.05	0.13
Na_2O	6.79	6.90	6.93	7.02	6.97	7.65	7.60	7.30	7.56	7.3	7.69	7.41	7.29	7.53	7.33
K_2O	0.23	0.40	0.13	0.18	–	0.22	0.60	–	–	–	0.09	0.03	0.09	0.26	0.39
Total	97.20	97.08	97.71	97.40	97.79	97.00	98.01	98.00	97.90	97.80	98.02	97.49	97.70	97.70	98.01
							23O								
Si	7.78	7.73	7.82	7.80	7.83	7.78	7.85	7.81	7.82	7.80	7.83	7.81	7.82	7.87	7.83
Ti	–	–	–	–	–	–	0.01	–	0.01	–	–	0.04	–	–	0.01
Al	–	0.01	–	–	0.09	0.02	0.03	0.12	0.10	0.09	0.09	–	0.12	0.01	0.03
Fe^{3+}	2.41	2.48	2.32	2.33	2.28	2.19	1.97	2.17	2.07	2.25	2.03	2.17	2.17	2.05	2.14
Fe^{2+}	1.41	1.33	1.86	1.53	1.10	1.12	1.19	1.15	1.34	1.17	1.31	1.23	1.03	1.48	1.11
Mn	–	–	–	0.01	–	–	–	–	–	–	0.01	0.01	–	–	–
Mg	1.39	1.46	0.99	1.34	1.70	1.90	1.95	1.76	1.66	1.69	1.73	1.74	1.86	1.59	1.88
Ca	0.02	–	–	0.01	0.01	0.01	0.02	0.03	0.02	0.01	0.02	0.02	0.01	0.01	0.02
Na	1.94	1.98	2.00	2.01	1.95	2.17	2.13	2.04	2.13	2.05	2.16	2.09	2.03	2.14	2.05
K	0.04	–	0.02	0.03	–	0.04	0.11	–	–	–	0.02	0.01	0.02	0.05	0.07
X_{Fe}	0.51	0.48	0.66	0.54	0.39	0.37	0.38	0.40	0.45	0.41	0.43	0.41	0.36	0.48	0.37

with tetraferribiotite and celadonite. It is greenish (owing to the presence of Fe^{3+} in amounts of 2.74–3.01 wt %), which substitutes Al^{3+} at the T site (Table 4). This composition of the microcline was caused by the chemistry of the rock, namely, its richness in Fe^{3+} and a low alumina content.

Some rocks contain accessory apatite.

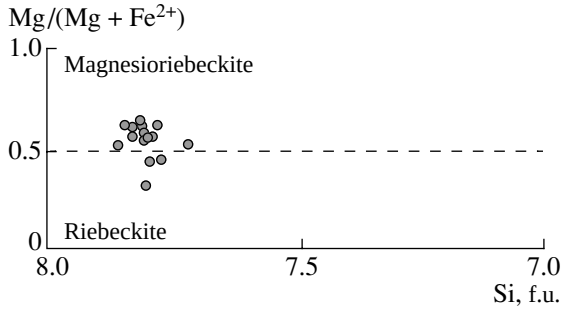

Fig. 9. Compositions of riebeckite from the Mikhailovskoe BIF shown in a classification plot.

METAMORPHIC *P–T* PARAMETERS

The rocks of the iron formation contain no minerals traditionally used as geothermometers and geobarometers. Moreover, there are no consistent thermodynamic data on many minerals of these rocks. Because of this, most researchers utilize thermobarometric estimates for the rocks hosting BIF, most often, metapelites. Earlier, in studying mineral equilibria in the chloritoid schists underlying BIF of the Stoilenskaya Formation, Kurskaya Group in the Mikhailovskii district, the following mineral assemblages were described: *Qtz* + *Cld* + *Chl*, *Qtz* + *Cld* + *Chl* + *Ms*, *Qtz* + *Cld* + *Chl* + *Ms* + *And*, and *Qtz* + *Cld* + *Grt* + *Chl* + *Ms* + *Bt* in the almandine–chlorite–chloritoid zone and *Qtz* + *St* + *Cld* + *Chl* + *Ms*, *Qtz* + *St* + *And* + *Cld* + *Chl* + *Bt* in the chloritoid–staurolite zone (Poskryakova, 2001). The appearance of staurolite in association with chloritoid in metapelites testifies for the transition from the almandine–chlorite–chloritoid zone of the greenschist facies to the staurolite–chlorite–chloritoid zone of the staurolite facies (Korikovsky, 1979). The *St* + *Cld* + *Bt* assemblage is stable over the temperature interval of 450–520°C at pressures of 2–3 kbar, according to the petrogenetic grid in (Spear and Cheney, 1989). Stauro-

Table 7. Chemical composition of aegirine in BIF from the Mikhailovskoe deposit

Component	3213/8	MK-18					3830/14			3195/15				
	29	21	22	23	28	31	47	48	50	60	62	64	66	70
	margin	margin	core	margin	core	margin	margin	core	margin	margin	margin	margin	core	margin
SiO_2	53.21	52.89	52.79	53.09	53.29	53.05	52.77	52.75	53.37	53.09	53.02	53.58	52.92	53.34
TiO_2	–	0.10	–	–	–	–	0.10	–	0.02	0.03	0.02	0.12	0.04	0.02
Al_2O_3	0.02	0.23	0.06	0.11	0.11	0.09	0.14	0.21	0.15	0.09	0.17	0.10	0.21	0.05
FeO	32.57	32.90	31.82	32.11	32.52	32.95	31.47	32.23	32.67	31.69	32.13	32.20	32.72	32.97
MnO	–	0.21	0.04	–	0.02	–	0.15	–	0.13	–	0.14	–	–	–
MgO	0.02	0.14	0.04	0.02	0.05	–	0.03	–	–	–	0.07	0.17	0.04	–
CaO	0.14	0.15	0.18	0.08	0.05	0.19	0.19	0.31	0.02	0.23	0.19	0.23	0.31	0.19
Na_2O	13.21	13.34	15.01	14.42	13.95	13.65	15.00	14.37	13.62	14.80	14.26	13.55	13.63	13.37
K_2O	–	–	0.05	–	–	0.03	0.01	0.07	0.01	0.05	0.03	–	0.01	0.03
Total	99.17	99.96	99.99	99.83	99.99	100.00	99.86	99.94	99.99	99.98	100.03	99.95	99.98	99.97
Si	2.00	1.98	1.94	1.96	1.98	1.98	1.94	1.95	1.99	1.95	1.96	1.99	1.97	1.99
Ti	–	–	–	–	–	–	–	–	–	–	–	–	–	–
Al	–	0.01	–	–	–	–	0.01	0.01	0.01	–	0.01	–	0.01	–
Fe^{3+}	0.95	1.00	1.19	1.10	1.04	1.03	1.18	1.12	1.00	1.14	1.09	0.97	1.03	0.98
Fe^{2+}	0.07	0.03	–	–	–	–	–	–	0.02	–	–	0.03	–	0.05
Mn	–	0.01	–	–	–	–	–	–	–	–	–	–	–	–
Mg	–	0.01	–	–	–	–	–	–	–	–	–	0.01	–	–
Ca	0.01	0.01	0.01	–	–	0.01	0.01	0.01	–	0.01	0.01	0.01	0.01	0.01
Na	0.96	0.97	1.07	1.03	1.00	0.99	1.07	1.03	0.98	1.06	1.02	0.98	0.98	0.97
K	–	–	–	–	–	–	–	–	–	–	–	–	–	–

lite-free assemblages with chloritoid, chlorite, and muscovite are stable at 370–470°C within the andalusite stability field. It follows that the prograde *P–T* metamorphic path, inferred from the phase equilibria and mineralogical thermometric data, can be estimated at 370–520°C at 2–3 kbar.

PETROGENESIS

The wide occurrence of K- and Na-bearing minerals in rocks of the iron formation in the Mikhailovskii district suggests that the protoliths of these rocks were the products of sedimentation and diagenesis of iron–silicate gels rich in Na and K (French, 1973; Klein, 1974). When this material starts to crystallize during diagenesis, the diffusion of cations is activated, and Na and K can be accommodated in the structures of mica and riebeckite. Eugster (1969) suggested, by analogy with Pleistocene siliceous lacustrine deposits, that magadiite $NaSi_7O_{13} \cdot 3H_2O$ was the first to crystallize in the iron-formation deposits. As a consequence of reaction with Fe-bearing mixed-layer silicates, Na was released and gave rise to riebeckite (Miyano, 1982). The very low-temperature metamorphism produced disordered K-micas almost devoid of Al, and their decomposition resulted in celadonite and tetraferribiotite.

Conceivably, part of the riebeckite, celadonite, and tetraferribiotite could crystallize from alkali-bearing solutions that entered the rocks during their deformations. In the Early Proterozoic iron formation of KMA, limited alkaline metasomatism proceeded within zones permeable to fluid (such as zones of fracturing and intense tectonization). This is confirmed by the observations of Trendall and Blockley (1970) that riebeckite develops in the iron formations of western Australia in close relation with deformations. Glagolev (1966) noted that the activity of alkaline metasomatism in the KMA iron formation was generally not high. The BIF with aegirine and riebeckite fully preserved their characteristic structures (thin banding and crenulation) and bear no metasomatic bodies with massive or impregnated structures. The aegirine and riebeckite coexist with quartz, magnetite, hematite, micas, and carbonates, i.e., there are absolutely no monomineralic and bimineralic associations. Because of this, Glagolev (1966) referred to the limited alkaline metasomatism in BIF as alkaline metamorphism.

The stability of hematite and magnetite in the BIF mineral assemblages testifies to high values of oxygen

fugacity, close to the magnetite–hematite buffer. This is corroborated by the elevated X_{Mg} of the tetraferribiotite, celadonite, chlorite, and riebeckite, because, in the general case, the X_{Fe} of Fe–Mg silicates decreases with increasing oxygen fugacity. An elevated oxygen fugacity during the metamorphism and the low Al_2O_3 concentration in the rocks account for the fact that the Mikhailovskoe BIF contain minerals high in Fe^{3+}. For example, these rocks ubiquitously bear celadonite and tetraferribiotite, which seem to have been stable throughout the whole greenschist facies. Low-temperature iron formations elsewhere commonly contain stilpnomelane (Klein and Gole, 1981; Haase, 1982; Floran and Papike, 1978; and others). Although the metamorphic parameters of the Mikhailovskoe BIF are above the stability field of this mineral (approximately 470°C at 2–3 kbar; Miyano and Klein, 1989), the latter was likely not stable even at lower temperatures because of the low alumina concentrations in the rocks and their high Fe_2O_3/FeO ratios. This is confirmed by the absolute absence of grunerite, which is, along with other minerals, an inevitable product of stilpnomelane decomposition at low pressures (Miyano and Klein, 1989). In place of stilpnomelane, the rocks contain widespread tetraferribiotite and celadonite, which suggests an elevated K^+ activity in the fluid.

Instead of greenalite $Fe_6Si_4O_{10}(OH)_8$, a mineral common in BIF of low metamorphic grades, the Mikhailovskoe rocks contain its "oxidized" analogue ferrichamosite (Fe^{2+}_5 $Fe^{3+}[Fe^{3+}Si_3O_{10}](OH)_8$. Chlorites are generally rare in iron formations because of the low Al_2O_3 contents of the rocks (Laird, 1989) and are commonly represented by chamosite (Gole, 1980) and, more rarely, clinochlore and ripidolite (Klein, 1983; Miyano and Beukes, 1997), which crystallize at the lowest metamorphic grades and, perhaps, catagenesis.

MINERAL FACIES

The reaction texture, described above, of alkali-rich BIF at the Mikhailovskoe deposit can be interpreted with the aid of chemical reactions in the system Na_2O–K_2O–FeO–Fe_2O_3–SiO_2–CO_2–H_2O.

The replacement textures of tetraferribiotite by celadonite suggest the oxidation of the former according to the reaction

$$\begin{gathered} Bt + Qtz + 1/2O_2 \longrightarrow Sld + Hem \\ K(Fe^{2+}, Fe^{3+})_3[Fe^{3+}Si_3O_{10}](OH)_2 + SiO_2 \\ + 1/2O_2 \longrightarrow KFe^{3+}Fe^{2+}[Si_4O_{10}](OH)_2 + Fe_2O_3 \end{gathered} \quad (1)$$

or

$$\begin{gathered} Bt + Qtz + 1/3O_2 \longrightarrow Sld + 2/3Mag \\ K(Fe^{2+}, Fe^{3+})_3[Fe^{3+}Si_3O_{10}](OH)_2 + SiO_2 \\ + 1/3O_2 \longrightarrow KFe^{3+}Fe^{2+}[Si_4O_{10}](OH)_2 + 2/3Fe_3O_4, \end{gathered} \quad (2)$$

and, depending on the oxygen fugacity in discrete layers, hematite [at higher f_{O_2}, reaction (1)] or magnetite [at lower f_{O_2}, reaction (2)] are formed in the right-hand sides of the reactions.

Aegirine and riebeckite were never found in equilibrium relations and generally occur simultaneously very rarely. They usually compose discrete layers, which, however, can be not far from one another. Even if the two minerals occur in the same layer, riebeckite retrogressively replaces aegirine grains in margins and along cracks or is contained as inclusions in aegirine. Hematite in most rocks coexists with riebeckite in aegirine-free layers but can also be absent from them. Hence, the stability of aegirine or riebeckite in the iron formations is more probably controlled by the oxygen fugacity rather than the temperature of metamorphism

$$\begin{gathered} 4Rbk + 3O_2 \longrightarrow 8Aeg + 6Hem + 16Qtz + H_2O \\ 4Na_2(Fe^{3+}Fe^{2+})_5[Si_8O_{22}](OH)_2 + 3O_2 \\ \longrightarrow 8NaFe^{3+}[Si_2O_6] + 6Fe^{3+}_2O_3 + 16SiO_2 + 4H_2O. \end{gathered} \quad (3)$$

REGIME OF OXYGEN AND ALKALIS DURING METAMORPHISM

Riebeckite presence in iron formations is controlled by f_{O_2}, a_{Na^+}, and temperature (Miyano and Klein, 1983). Furthermore, if riebeckite occurs in assemblage with ankerite and/or siderite, its stability field expands with the increasing CO_2 activity in the fluid. The stability of riebeckite in iron formations cannot serve as an clear-cut indicator of the metamorphic temperature interval if other factors are not accounted for. Riebeckite (more specifically, its asbestiform variety crocidolite) can develop at the sacrifice of iron oxides, carbonates, and quartz at very low temperature metamorphism or even diagenesis, starting from 130°C, at the active interaction of Fe-rich rocks with Na^+-bearing solutions (Miyano and Klein, 1983).

Since aegirine and riebeckite rarely occur together in our rocks and compose different layers at the Mikhailovskoe deposit, it is reasonable to conclude that no reaction of high-temperature riebeckite decomposition with the origin of aegirine *Rbk* + *Hem* = *Aeg* + *Mag* + *Qtz* + H_2O took place. This makes it possible to constrain the upper temperature boundary of metamorphism. The position of reaction lines in the diagram was constrained experimentally (Ernst, 1962) and calculated (Miyano and Beukes, 1997). According to these data, high-temperature riebeckite decomposition with the origin of aegirine proceeds at 510–520°C, 2.5 kbar, and a_{H_2O} = 1.0 and is independent of oxygen fugacity and sodium activity in the fluid.

Our BIF never contain grunerite, but reaction relationships between grunerite and riebeckite were described in the Penge iron formation, South Africa,

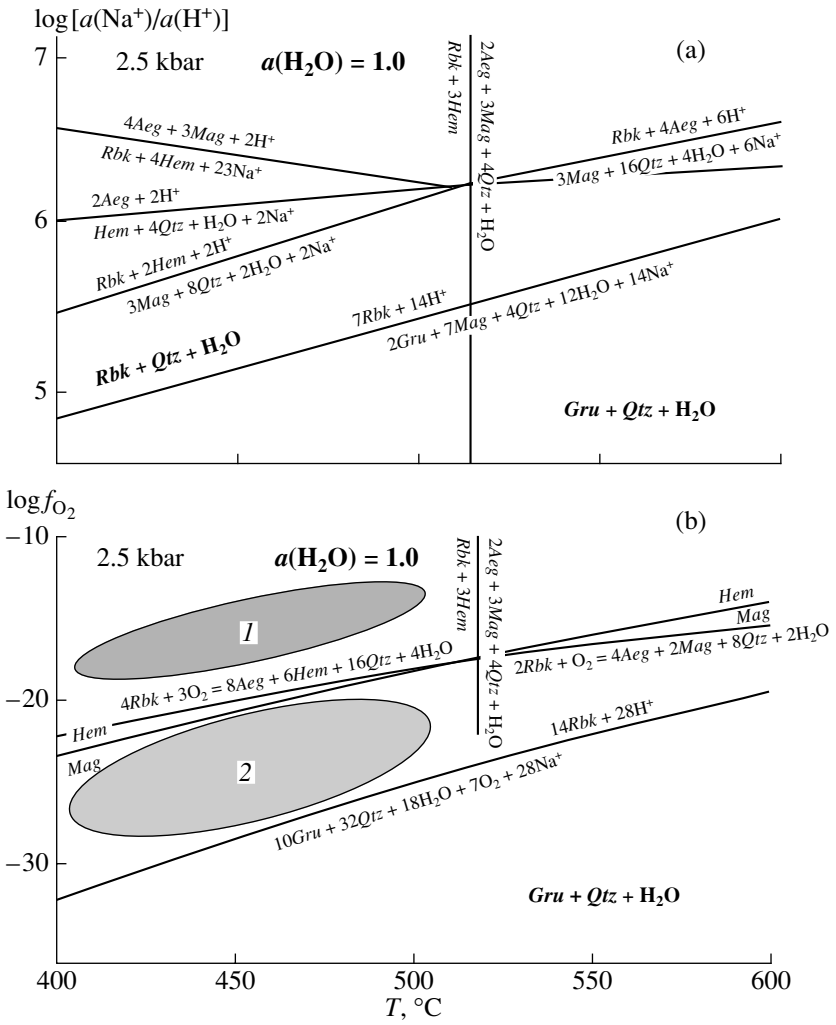

Fig. 10. Stability of riebeckite shown in (a) $[\log[a(Na^+)/a(H^+)]$ vs. *T* and (b) $\log[f_{O_2}]$ vs. *T* diagrams. Shaded fields correspond to: (*1*) stability of the *Rbk* + *Mag* assemblage and (*2*) stability of the *Aeg* + *Hem* assemblage, calculated for a pressure of 2.5 kbar and $a(H_2O) = 1.0$ (according to Miyano and Beukes, 1997).

(Miyano and Beukes, 1997) and the Prioskol'skoe iron deposit of KMA (Savko and Kal'mutskaya, 2002). Miyano and Beukes (1997) calculated the position of the reaction *Gru* + *Mag* + *Qtz* + H_2O = *Rbk* in a $\log[a(Na^+)/a(H^+)]$ vs. *T* as a function of the Na activity in the fluid. According to the data of these researchers, riebeckite is stable instead of grunerite at a high Na activity, $[\log[a(Na^+)/a(H^+) > 5.0–5.5$ over the temperature interval of 400–500°C (Fig. 10). At a higher Na activity, riebeckite should decompose and produce aegirine by the reaction *Rbk* + *Hem* + Na^+ = *Aeg* + *Mag* + H^+, which proceeds at $\log[a(Na^+)/a(H^+) = 6.5$ at 400°C. No such reaction took place in our rocks, because they contain aegirine, but not riebeckite, in association with hematite. Hence, metamorphic transformations of the Mikhailovskoe iron formations occurred at a high Na activity in the fluid at $\log[a(Na^+)/a(H^+)] = 5.0–6.5$ (Fig. 10).

According to Miyano and Beukes (1997), aegirine forms at the expense of riebeckite by the following reactions at different metamorphic regimes:

Rbk + 3*Hem* = 2*Aeg* + 3*Mag* + 4*Qtz* + H_2O if the temperature increases;

2*Rbk* + O_2 = 4*Aeg* + 2*Mag* + 8*Qtz* + $2H_2O$ if the oxygen fugacity increases;

Na^+ – *Rbk* + 4*Hem* + $23Na^+$ = 4*Aeg* + 3*Mag* + $2H^+$ if the sodium activity increases.

The latter reaction producing magnetite and aegirine occurs in the high-temperature region, at temperatures above 510°C (Miyano and Beukes, 1997). It follows that the only plausible mechanism forming aegirine from riebeckite in our BIF is reaction (3): 4*Rbk* + $3O_2 \longrightarrow$ 8*Aeg* + 6*Hem* + 16*Qtz* + $4H_2O$, which is

controlled by the redox conditions of metamorphism. The position of this reaction in a $\log(f_{O_2}) - T\,^\circ C$ space calculated for 2.5 kbar and $a_{H_2O} = 1$ nearly coincides with the hematite–magnetite buffer over the temperature interval of 400–500°C (Miyano and Beukes, 1997). Hence, the occurrence of aegirine or riebeckite in the alkali-rich BIF at KMA is a sensitive indicator of oxygen fugacity during metamorphism (Fig. 10).

In most Precambrian iron formations, oxygen behaves as a locally dependent (inert) component (Frost, 1982; Fonarev, 1987; Savko, 1994). Many researchers admit that oxygen fugacity in metamorphic iron formations depends on its original concentration in them (Korzhinskii, 1940; Marakushev, 1965) and can only little vary during metamorphism because of the inert behavior of this element. In every area or even an individual layer, oxygen fugacity is controlled by the conditions of sedimentation and diagenesis and by buffer reactions. Because of this, oxygen fugacity may vary from layer to layer even within a single iron formation but is thought to remain constant within the layers. This is usually manifested in variations in the X_{Fe} of silicates from layer to layer in the iron formations, for example, these parameters of grunerite and orthopyroxene in the presence of hematite or magnetite. In the alkali-rich iron formations of KMA, the variations in the oxygen fugacity between individual layers are reflected in the stability of the *Aeg + Hem* and *Rbk + Mag* assemblages.

CONCLUSIONS

The early Proterozoic iron formations of the Mikhailovskoe deposit at KMA contain widespread K-bearing, Al-free micas (tetraferribiotite and celadonite), carbonates (ankerite and siderite), riebeckite, and aegirine. Studying the mineral equilibria in the rocks enables reproducing the genetic successions of mineral assemblages and the physicochemical parameters of metamorphism. Early in the course of metamorphic processes, the rocks contained quartz, carbonates, iron oxides, specific K-bearing and Al-free micas, and Fe-rich and Al-free chlorite. Later, depending on the oxygen fugacity in individual layers (above or below the hematite–magnetite buffer), the *Aeg + Hem* or *Rbk + Mag* assemblages developed. The metamorphic temperature is estimated at 370–520°C at pressures of 2–3 kbar, $\log[a(Na^+)/a(H^+)] = 5.5–6.0$, and an oxygen fugacity above the hematite–magnetite buffer in layers containing the *Aeg + Hem* assemblage and below this buffer in layers with the *Rbk + Mag* assemblage.

ACKNOWLEDGMENTS

The authors thank S.P. Korikovsky (Institute of the Geology of Ore Deposits, Petrography, Mineralogy, and Geochemistry, Russian Academy of Sciences) for constructive criticism and valuable comments during the preparation of the manuscript; V.A. Skulkov (Yugozapadgeologiya Geological Survey) and V.N. Babanskii (Mikhailovskii Mining and Processing Enterprise) for help with the fieldwork. This study was financially supported by Russian Universities Grant (project UR.09.01.038), the Russian Foundation for Basic Research (project nos. 03-05-64071, 03-05-79088), President of the Russian Federation (project MD-428.2003.05), and the Integration Federal Program (project E0348).

REFERENCES

Burt, D.M., Vector Representation of Phyllosilicate Compositions, *Rev. Mineral.*, 1989, vol. 19, part 14, pp. 584–599.

Ernst, W.G., Synthesis, Stability Relations, and Occurrence of Ribeckite and Ribeckite–Arfvedsonite Solid Solutions, *J. Geol.*, 1962, vol. 70, pp. 689–736.

Eugster, H.P., Inorganic Bedded Cherts from the Magadi Area, Kenya, *Contrib. Mineral. Petrol.*, 1969, vol. 22, pp. 1–31.

Floran., R.J. and Papike, J.J., Mineralogy and Petrology of the Gunflint Iron Formation, Minnesota–Ontario: Correlation of Compositional and Assemblage Variations at Low to Moderate Grade, *J. Petrol.*, 1978, vol. 19, pp. 215–288.

Fonarev, V.I., *Mineral'nye ravnovesiya zhelezistykh formatsii dokembriya* (Mineral Equilibria in Precambrian BIF), Moscow: Nauka, 1987.

Foster, M.D., Green Mica from BIF of the Kursk Magnetic Anomaly, *Zap. Vses. Mineral. O–va*, 1959, part 88, no. 6, pp. 729–730.

French, B.M., Mineral Assemblages in Diagenetic and Low-Grade Metamorphic Iron Formations, *Econ. Geol.*, 1973, vol. 68, pp. 1063–1074.

Frost, B.R., Contact Metamorphic Effect of the Stillwater Complex, Montana: The Concordant Iron Formation: A Discussion of the Role of Buffering in Metamorphism of Iron Formation, *Am. Mineral.*, 1982, vol. 67, no. 1/2, pp. 142–148.

Glagolev, A.A., *Metamorfizm dokembriiskikh porod KMA* (Metamorphism of the Kursk Magnetic Anomaly Precambrian Rocks), Moscow: Nauka, 1966.

Gole, M.J. and Klein, C., Banded Iron Formation through Much of Precambrian Time, *J. Geol.*, 1981, vol. 89, pp. 169–183.

Gole, M.J., Mineralogy and Petrology of Very Low-Grade Metamorphic Archean Banded Iron Formations, Weld Range, Western Australia, *Am. Mineral.*, 1980, vol. 65, pp. 8–25.

Haase, C.S., Metamorphic Petrology of the Negaunee Iron Formation, Marquette District, Northern Michigan: Mineralogy, Metamorphic Reactions, and Phase Equilibria, *Econ. Geol.*, 1982, vol. 77, pp. 60–81.

Illarionov, A.A., *Petrografiya i mineralogiya zhelezistykh kvartsitov Mikhailovskogo mestorozhdeniya Kurskoi magnitnoi anomalii* (Petrography and Mineralogy of BIF from Mikhailovskoe Deposit, Kursk Magnetic Anomaly), Moscow: Nauka, 1965.

James, H.L., Sedimentary Facies of Iron Formation, *Econom. Geol.*, 1954, vol. 49, pp. 235–285.

Klein, C., Mineralogy and Petrology of the Metamorphosed Wabush Iron Formation, Southwestern Labrador, *J. Petrol.*, 1966, vol. 7, pp. 246–305.

Klein, C., Changes in Mineral Assemblages with Metamorphism of Some Banded Precambrian Iron Formations, *Econ. Geol.*, 1973, vol. 68, pp. 1075–1088.

Klein, C., Greenalite, Minnesotaite, Crocidolite, and Carbonates in a Very Low-Grade Metamorphic Precambrian Iron Formation, *Can. Mineral.*, 1974, vol. 12, pp. 475–498.

Klein, C. and Gole, M.J., Mineralogy and Petrology of Parts of the Marra Mamba Iron Formation, Hamersley Basin, Western Australia, *Am. Mineral.*, 1981, vol. 66, pp. 507–525.

Klein, C., *Diagenesis and Metamorphism of Precambrian Iron Formations*, Trendall, A.F. and Morris, R.C., Eds., Amsterdam: Elsevier, 1983, pp. 417–469.

Korikovsky, S.P., *Fatsii metamorfizma metapelitov* (Facies of Metapelite Metamorphism), Moscow: Nauka, 1979.

Korzhinskii, D.S., *Faktory mineral'nykh ravnovesii i mineralogicheskie fatsii glubinnosti* (Factors of Mineral Equilibria and Mineralogical Facies of Depth), Moscow: Akad. Nauk SSSR, 1940, issue 12, no. 5.

Laird, J., Chlorites: Metamorphic Petrology, *Rev. Miner.*, 1989, vol. 19, Cpt. 11, pp. 405–453.

Leake, B.E., Woolley, A.R., and 20 Members of the Subcommittee on Amphiboles, Nomenclature of Amphiboles. Report of the Subcommittee on Amphiboles of the International Mineralogical Association Commission on New Minerals and Mineral Names, *Eur. J. Miner.*, 1997, vol. 9, pp. 623–651.

Marakushev, A.A., *Problemy mineral'nykh fatsii metamorficheskikh i metasomaticheskikh porod* (Problems of the Mineral Facies of Metamorphic and Metasomatic Rocks), Moscow: Nauka, 1965.

Miyano, T., Stilpnomelane, Fe-Rich Mica, K-Feldspar, and Hornblende in Banded Iron Formation Assemblages of the Dales Gorge Member, Hammersley Group, Western Australia, *Can. Mineral.*, 1982, vol. 20, pp. 189–202.

Miyano, T. and Beukes, N.J., Mineralogy and Petrology of the Contact Metamorphosed Amphibole Asbestos-Bearing Penge Iron Formation, Eastern Transvaal, South Africa, *J. Petrol.*, 1997, vol. 38, no. 5, pp. 651–676.

Miyano, T. and Klein, C., Conditions of Riebeckite Formation in the Iron Formation of the Dales Gorge Member, Hamersley Group, Western Australia, *Am. Mineral.*, 1983, vol. 68, pp. 517–529.

Miyano, T. and Klein, C., Phase Equilibria in the System K_2O–FeO–MgO–Al_2O_3–SiO_2–CO_2–H_2O and the Stability Limit of Stilpnomelane in Metamorphosed Precambrian Iron Formations, *Contrib. Mineral. Petrol.*, 1989, vol. 102, pp. 478–491.

Miyano, T. and Miyano, S., Ferri-Annite from the Dales George Member Iron Formations, Wittenoom Area, Western Australia, *Am. Mineral.*, 1982, vol. 67, pp. 1179–1194.

Poskryakova, M.V., *Fazovye ravnovesiya na granitse zelenoslantsevoi i stavrolitovoi fatsii metamorfizma na primere Mikhailovskogo rudnogo raiona KMA* (Phase Equilibria at the Boundary between the Greenschist and Staurolite Facies of Metamorphism with Reference to the Mikhailovskii Ore Field, Kursk Magnetic Anomaly), *Vestn. Voronezh. Univ., Geologiya*, 2001, issue 11, pp. 122–131.

Rieder, M. *et al.*, Nomenclature of the Micas, *Mineral. Mag.*, 1999, vol. 63(2), pp. 267–279.

Robinson, P., Spear, F.S., *et al.*, Phase Relations of Metamorphic Amphiboles: Natural Occurrence and Theory, *Rev. Mineral.*, 1982, vol. 9, pp. 3–227.

Savko, K.A., Fayalite–Grunerite–Magnetite–Quartz Rocks in BIF of the Voronezh Crystalline Massif: Phase Equilibria and Metamorphic Conditions, *Petrologiya*, 1994, vol. 2, no. 5, pp. 540–550.

Savko, K.A., Physicochemical Parameters of Metamorphism of Eulysites from the Central Part of the Voronezh Crystalline Massif, *Vestn. Voronezh. Univ., Geol.*, 1999, no. 8, pp. 73–81.

Savko, K.A. and Kal'mutskaya, N.Yu., Physicochemical Conditions of Metamorphism of Magnetite–Grunerite–Riebeckite Rocks at the Prioskol'skoe Iron Deposit, Kursk Magnetic Anomaly, *Vestn. Voronezh. Univ., Geol.*, 2002, no. 1, pp. 95–103.

Shchegolev, I.N., *Zhelezorudnye mestorozhdeniya dokembriya i metody ikh izucheniya* (Precambrian Iron Deposits and Methods of Their Study), Moscow: Nedra, 1985.

Spear, F.S. and Cheney, J.T., A Petrogenetic Grid for Pelitic Schists in the System SiO_2–Al_2O_3–FeO–MgO–K_2O–H_2O, *Contrib. Mineral. Petrol.*, 1989, vol. 101, no. 29, pp. 149–164.

Sudovikova, E.N., Green Mica from the Iron Ore Sequence of the Kursk Magnetic Anomaly, *Zap. Vses. Mineral. O–va*, 1956, part. 85, no. 4, pp. 543–549.

Trendall, A.F. and Blockley, J.G., The Iron Formation of the Precambrian Hamersley Group, Western Australia, with Special Reference to the Associated Crocidolite, *Western Australia Geol. Surv. Bull.*, 1970, p. 119.

Veres, G.I., Merenkova, T.B., and Ostrovskii, I.A., Artificial Pure Ferrous Hydroxyl Mica, *Dokl. Akad. Nauk SSSR*, 1955, vol. 101, no. 1, pp. 147–150.

Wones, D.R., Phase Equilibria of "Ferriannite," $K Fe_3^{+2} Fe^{+3} Si_3 O_{10}(OH)_2$, *Am. J. Sci.*, 1963, vol. 261, pp. 581–596.